New Journal of Physics
The open–access journal for physics

Next generation double-beta decay experiments: metrics for their evaluation

F T Avignone III[1], G S King III[1] and Yu G Zdesenko[2,3]

[1] Department of Physics and Astronomy, University of South Carolina Columbia, SC 29208, USA

[2] Institute for Nuclear Research, Kiev, Ukraine

E-mail: avignone@sc.edu

New Journal of Physics **7** (2005) 6

Received 03 September 2004

Published 12 January 2005

Online at http://www.njp.org/

doi:10.1088/1367-2630/7/1/006

Abstract. We discuss the six most important parameters that should be used in the computation of figures of merit of various proposed searches for neutrinoless double-beta decay ($0\nu\beta\beta$-decay). We begin by discussing the connection of this decay mode to the effective Majorana mass of the electron neutrino and the expected experimental sensitivities of favoured techniques. We then discuss the proposed next generation $0\nu\beta\beta$-decay experimental techniques in the context of an expression for the experimental figure-of-merit. Finally, we discuss the various proposed experiments in the context of their figure-of-merit parameters. We conclude that the important parameters are the nuclear structure (theoretical rate of decay), isotopic abundance of the parent nuclide and detection efficiency for $0\nu\beta\beta$-decay. These enter the equation linearly. Also important are: the mass of the source, and the background rate, although these enter to the one-half power. Energy resolution, while also entering the figure-of-merit to the one half power, is crucial for the discovery potential.

[3] Deceased.

PII: S1367-2630(05)85887-2

Contents

1. Theoretical background

1.1. Theoretical motivation of $0\nu\beta\beta$-decay

Neutrinoless double-beta decay is an old subject [16, 34, 35, 41, 63, 71, 72, 82]. What is new is the fact that positive observation of neutrino oscillations in atmospheric neutrinos [37] and in solar neutrinos [6, 36] gives new motivation for more sensitive searches. In fact, recently published constraints on the mixing angles of the neutrino-mixing matrix [18, 67, 68] make a strong case that if neutrinos are Majorana particles, there are many scenarios in which next generation double-beta decay experiments should be able to observe the phenomenon and measure the effective Majorana mass of the electron neutrino, $|\langle m_\nu \rangle|$, which would provide a measure of the neutrino mass scale. One fact is clear; neutrino oscillation experiments can only provide data on the mass differences of the neutrino mass-eigenstates. The absolute scale can only be obtained from direct mass measurements, ^3H end point measurements for example [66], or in the case of Majorana neutrinos, more sensitively by neutrinoless double-beta decay. The time for large, next generation double beta-decay experiments has arrived, for if the mass scale is below $\sim$0.2 eV, double beta-decay may be the only hope for measuring it. The most sensitive experiments carried out so far have probed the decay $^{76}\mathrm{Ge} \rightarrow {}^{76}\mathrm{Se} + 2\beta^-$ with specially built Ge detectors fabricated from germanium isotopically enriched from 7.8 to 86% in ^{76}Ge. The Heidelberg–Moscow Experiment [20, 49] and the International Germanium Experiment (IGEX) [2, 4] have placed lower bounds on the half-life for this process of 1.9×10^{25} years (90% CL) and 1.6×10^{25} years (90% CL), respectively.

1.2. The neutrino mixing matrix

The conventional form of the Kobayashi–Maskoawa matrix was suggested by Chau and Keung in 1984 [26].

$$\begin{pmatrix} |\nu_e\rangle \\ |\nu_\mu\rangle \\ |\nu_\tau\rangle \end{pmatrix} = \begin{pmatrix} c_3c_2 & s_3c_2 & s_2e^{-i\delta} \\ -s_3c_1 - c_3s_1s_2e^{i\delta} & c_3c_1 - s_3s_1s_2e^{i\delta} & s_1c_2 \\ s_3s_1 - c_3s_1s_2e^{i\delta} & -c_3s_1 - s_3c_1s_2e^{i\delta} & c_1c_2 \end{pmatrix} \begin{pmatrix} 1 & 0 & 0 \\ 0 & e^{i\varphi_2/2} & 0 \\ 0 & 0 & e^{i(\delta+\varphi_2/2)} \end{pmatrix} \begin{pmatrix} |\nu_1\rangle \\ |\nu_2\rangle \\ |\nu_3\rangle \end{pmatrix}, \tag{1}$$

where $c_i \equiv \cos\theta_i$ and $s_i \equiv \sin\theta_i$, and we multiply by an additional diagonal matrix that contains Majorana CP phases that do not appear in neutrino oscillations. While this looks very complicated and populated with many unknowns, neutrino oscillation data [6, 10, 36, 45] have constrained all three of the angles as shown in table 1.

In addition, these experiments have produced limits of $10^{-5}\,\mathrm{eV}^2 \leqslant \delta m_S^2 \leqslant 10^{-4}\,\mathrm{eV}^2$ (3σ) for solar neutrino oscillations and $1.1\times10^{-3}\,\mathrm{eV}^2 \leqslant \delta m_{AT}^2 \leqslant 5\times10^{-3}$ (3σ) for atmospheric neutrino oscillations. Considering the values found in table 1, one may wish to make the approximation that $\theta_2 \equiv 0$. Accordingly,

$$U = \begin{pmatrix} c_3 & s_3e^{i\varphi_2} & 0 \\ -s_3c_1 & c_3c_1e^{i\varphi_2} & s_1e^{i\varphi_3} \\ s_3s_1 & -c_3s_1e^{i\varphi_2} & c_1e^{i\varphi_3} \end{pmatrix} \simeq \begin{pmatrix} \frac{\sqrt{3}}{2} & \frac{1}{2}e^{i\varphi_2} & 0 \\ -\frac{1}{2\sqrt{2}} & \frac{\sqrt{3}}{2\sqrt{2}}e^{i\varphi_2} & \frac{1}{\sqrt{2}}e^{i\varphi_3} \\ \frac{1}{2\sqrt{2}} & -\frac{\sqrt{3}}{2\sqrt{2}}e^{i\varphi_2} & \frac{1}{\sqrt{2}}e^{i\varphi_3} \end{pmatrix}, \tag{2}$$

where $c_3 \cong \sqrt{3}/2$, $s_3 \simeq 1/2$ and $c_1 \simeq 1/\sqrt{2} = s_1$ were used in the second matrix.

Table 1. Atmospheric, reactor, and solar neutrino constraints on the mixing angles of equation (1).

Atmospheric neutrino data	Solar neutrino data	
(Super Kamiokande detector) [37]	Sudbury neutrino Observatory [6]	Super Kamiokande [36]
$s_1 \geqslant 0.0557$ (3σ); $\theta_1 \geqslant 34^\circ$	$0.794 \leqslant c_3 \leqslant 0.905$	$0.769 \leqslant c_3 \leqslant 0.894$
Reactor experiments:	Best fit $\theta_3 = 32^\circ$	$0.447 \leqslant s_3 \leqslant 0.639$
(CHOOZ and Palo Verde)		
$s_2 \leqslant 0.16$; $0.987 \leqslant c_2 \leqslant 1.00$	$c_3 = 0.866^{+0.039}_{-0.072}$ (3σ)	$17^\circ \leqslant \theta_3 \leqslant 39^\circ$
CL = 95% [10, 24]	$s_3 = 0.50^{+0.11}_{-0.07}$ (3σ)	$\theta_3 \approx 33^\circ$
KAMLAND	Best fit $\theta_3 = 32.6^\circ$ [46]	

There have been a series of reanalyses of both solar and atmospheric neutrino oscillations. A recent global analysis of all available data was presented by M C Gonzales-Garcia on 12 February 2004 at the International Workshop on 'Neutrino Oscillations and their Origins', NOON 2004 in Tokyo. The following neutrino mixing matrix was derived from that presentation.

The error bars were obtained by using the best-fit values as central ones, and computing 1σ errors from the 3σ ranges given.

$$\begin{pmatrix} U_{e1} & U_{e2} & U_{e3} \\ U_{\mu 1} & U_{\mu 2} & U_{\mu 3} \\ U_{\tau 1} & U_{\tau 2} & U_{\tau 3} \end{pmatrix} = \begin{pmatrix} 0.83 \pm 0.02 & 0.55 \pm 0.03 & < 0.23 \\ 0.37 \pm 0.06 & 0.57 \pm 0.06 & 0.70 \pm 0.04 \\ 0.36 \pm 0.06 & 0.56 \pm 0.05 & 0.69 \pm 0.05 \end{pmatrix}. \tag{3}$$

1.3. Neutrinoless double-beta decay

The decay rate for the process involving the exchange of the Majorana neutrino in the absence of right-handed currents, can be expressed as follows (for details see [35, 41]):

$$(T_{1/2})^{-1} = G^{0\nu}(E_0, Z) \left(\frac{\langle m_\nu \rangle}{m_e} \right)^2 |M_f^{0\nu} - (g_A/g_V)^2 M_{GT}^{0\nu}|^2. \tag{4}$$

In equation (4), $G^{0\nu}$ is the two-body phase-space factor including coupling constants, $M_f^{0\nu}$ and $M_{GT}^{0\nu}$ are the Fermi and Gamow–Teller nuclear matrix elements, respectively, and g_A and g_V are the axial-vector and vector relative weak coupling constants, respectively. The quantity $|\langle m_\nu \rangle|$ is the effective Majorana electron neutrino mass given by

$$|\langle m_\nu \rangle| \equiv ||U_{e1}^L|^2 m_1 + |U_{e2}^L|^2 m_2 e^{i\phi_2} + |U_{e3}^L|^2 m_3 e^{i\phi_3}|, \tag{5}$$

where $e^{i\phi_2}$ and $e^{i\phi_3}$ are the Majorana CP phases (± 1 for CP conservation) and $m_{1,2,3}$ are the neutrino mass eigenvalues. In general, prior to the approximation $\theta_2 = 0 = s_2$, we have

$$|\langle m_\nu \rangle| = |c_3^2 c_2^2 m_1 + s_3^2 c_2^2 e^{i\phi_2} m_2 + s_2^2 e^{i\phi_3} m_3|. \tag{6}$$

With the values and errors (1σ) from equation (3), this becomes:

$$|\langle m_\nu \rangle| = |(0.70 \pm 0.03) m_1 + (0.30 \pm 0.03) e^{i\phi_2} m_2 + (< 0.05) e^{i\phi_3} m_3|. \tag{7}$$

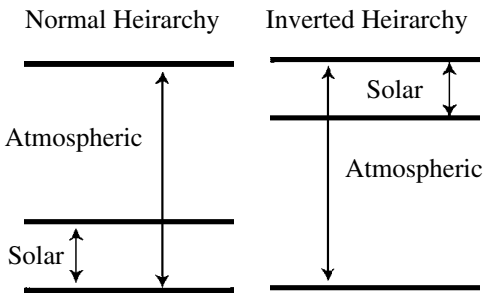

Figure 1. Normal and inverted hierarchies of the neutrino eigenstates. In the normal case, the solar neutrino oscillation occurs between the lower two states, and the atmospheric neutrino oscillation occurs between the highest and one of the lower ones. For convenience, we choose the lowest one to be m_1.

1.4. Neutrino mass patterns

The measured values of δm_S^2 (solar) and δm_{AT}^2 (atmospheric) given earlier motivate the pattern of masses in two hierarchy schemes shown in figure 1.

From the relations shown in figure 1, we can write $m_2 = \sqrt{\delta m_S^2 + m_1^2}$ and $m_3 = \sqrt{\delta m_{AT}^2 + m_1^2}$ in the case of normal hierarchy and $m_2 = \sqrt{\delta m_{AT}^2 - \delta m_S^2 + m_1^2}$ and $m_3 = \sqrt{\delta m_{AT}^2 + m_1^2}$ in the case if inverted hierarchy. From these, we can write equation (6), for normal and inverted hierarchy, respectively, in terms of mixing angles, δm_S^2, δm_{AT}^2 and CP phases as follows [17, 19, 67, 68]:

$$|\langle m_\nu \rangle| = \left| c_2^2 c_3^2 m_1 + c_2^2 s_3^2 \mathrm{e}^{\mathrm{i}\phi_2} \sqrt{\delta m_s^2 + m_1^2} + s_2^2 \mathrm{e}^{\mathrm{i}\phi_3} \sqrt{\delta m_{AT}^2 + m_1^2} \right|, \tag{8}$$

$$|\langle m_\nu \rangle| = \left| s_2^2 m_1 + c_2^2 c_3^2 \mathrm{e}^{\mathrm{i}\phi_2} \sqrt{\delta m_{AT}^2 - \delta m_s^2 + m_1^2} + c_2^2 s_2^2 \mathrm{e}^{\mathrm{i}\phi_3} \sqrt{\delta m_{AT}^2 + m_1^2} \right|. \tag{9}$$

With the approximation $\theta_2 \equiv 0$, and the further approximation of $\delta m_S^2 \ll \delta m_{AT}^2$, equations (8) and (9) are rewritten as follows in equations (10) and (11), respectively:

$$|\langle m_\nu \rangle| = m_1 \left| c_3^2 + s_3^2 \mathrm{e}^{\mathrm{i}\phi_2} \left(1 + \frac{\delta m_s^2}{2 m_1^2} \right) \right|, \tag{10}$$

$$|\langle m_\nu \rangle| = \sqrt{m_1^2 + \delta m_{AT}^2} \left| c_3^2 \mathrm{e}^{\mathrm{i}\phi_2} + s_3^2 \mathrm{e}^{\mathrm{i}\phi_3} \right|. \tag{11}$$

When the approximate expressions (10) and (11) are used, the results for equation (10) deviate from those using equation (8) by 2.5, 0.25 and 0.03% for $m_1 = 0.01, 0.02$ and 0.03 eV, respectively. In the case of using equation (11) for equation (9), the deviations are 1.4, 1.3 and 1.2% for $m_1 = 0.00$, 0.01 and 0.02 eV, respectively. Numerical values for $|\langle m_\nu \rangle|$ using equations (10) and (11) are given in table 2.

1.5. Experimental prospects

It is interesting to compare the values given in table 2 with the projected sensitivity of a 500 kg ^{76}Ge experiment for example. A projected sensitivity, for such an experiment would

Table 2. Numerical predictions of $|\langle m_\nu\rangle|$ in meV for both hierarchies and CP phase relations. (The errors are actually limits obtained by using the 3σ bounds on the measured parameters.)

Normal hierarchy				Inverted hierarchy			
$e^{i\phi_2} = -1$		$e^{i\phi_2} = +1$		$e^{i\phi_2} = -e^{i\phi_3}$		$e^{i\phi_2} = +e^{i\phi_3}$	
m_1(eV)	$\lvert\langle m_\nu\rangle\rvert$	m_1(eV)	$\lvert\langle m_\nu\rangle\rvert$	m_1(eV)	$\lvert\langle m_\nu\rangle\rvert$	m_1(eV)	$\lvert\langle m_\nu\rangle\rvert$
0.02	10^{+3}_{-5}	0.02	20 ± 4	0.00	30^{+18}_{-20}	0.00	55 ± 29
0.04	20^{+6}_{-10}	0.04	40 ± 8	0.02	32^{+18}_{-21}	0.02	59 ± 29
0.06	32^{+7}_{-16}	0.06	61 ± 11	0.05	40^{+18}_{-25}	0.05	75 ± 29
0.08	41^{+10}_{-21}	0.08	81 ± 16	0.075	48^{+19}_{-29}	0.075	94 ± 30
0.10	51^{+13}_{-26}	0.10	101 ± 20	0.10	60^{+19}_{-33}	0.10	116 ± 31
0.20	102^{+26}_{-52}	0.20	200 ± 40	0.20	106^{+30}_{-55}		
0.40	204^{+52}_{-102}	0.40	400 ± 80				

Table 3. Nuclear factors for neutrinoless double-beta decay of ^{76}Ge from 1998–2001.

Renormalized QRPA (Simcovic *et al*)	$F_N^{-1/2} = 4.02 \times 10^6$ (year)$^{1/2}$
SQRPA large basis (Heidelberg H V K-K)	$F_N^{-1/2} = 3.93 \times 10^6$ (year)$^{1/2}$
SQRPA small basis (Heidelberg H V K-K)	$F_N^{-1/2} = 3.33 \times 10^6$ (year)$^{1/2}$
SQRPA (J Suhonen)	$F_N^{-1/2} = 3.02 \times 10^6$ (year)$^{1/2}$
$\langle F_N^{-1/2}\rangle = (3.6 \pm 0.8) \times 10^6$ (year)$^{1/2}$	

be: $T^{0\nu}_{1/2} \geqslant 4 \times 10^{27}$ years [60]. To do this, we need the nuclear structure factor in equation (4). It is convenient to define $F_N \equiv G^{0\nu}|M^{0\nu}_f - (g_A/g_V)^2 M^{0\nu}_{GT}|^2$ which leads to $|\langle m_\nu\rangle| = m_e(F_N T^{0\nu}_{1/2})^{-1/2}$ eV.

In table 3, we list a few recent values of $F_N^{-1/2}$ (year)$^{1/2}$ calculated by three different Quasi-Particle Random Phase Approximation (QRPA) models.

Using the average value of those given in table 3 and the mean-square deviation, we find that experiment predicts a sensitivity of $|\langle m_\nu\rangle|_{SENS} \cong 28^{+7}_{-6}$ meV. This value probes a significant portion of the range of values of m_1 given in the table. The Cryogenic Underground Observatory for Rare Events (CUORE) experiment [13] will probe a similar range. The equations given by Barger *et al* [19] reduce, using the approximations given above, to the following for normal and inverted hierarchies respectively:

$$|\langle m_\nu\rangle| \leqslant m_1 \leqslant \frac{|\langle m_\nu\rangle|}{c_3^2 - s_3^2}, \tag{12}$$

$$\sqrt{|\langle m_\nu\rangle|^2 + \delta m^2_{AT}} \leqslant m_1 \leqslant \frac{\sqrt{|\langle m_\nu\rangle|^2 + \delta m^2_{AT}(c_3^2 - s_3^2)}}{c_3^2 - s_3^2}. \tag{13}$$

They also derive explicit expressions for $\sum \equiv m_1 + m_2 + m_3$, the sum of the eigenstate masses, which is important in the consideration of neutrino hot dark matter [19].

$$2|\langle m_\nu\rangle|^2 + \sqrt{|\langle m_\nu\rangle|^2 \pm \delta m^2_{AT}} \leqslant \sum \leqslant \frac{2|\langle m_\nu\rangle| + \sqrt{|\langle m_\nu\rangle|^2 \pm \delta m^2_{AT}\cos(2\theta_3)}}{\cos(2\theta_3)}, \tag{14}$$

where the plus is for normal hierarchy and the minus for inverted hierarchy. Equation (14) can be simplified significantly for values of $|\langle m_\nu\rangle|$ achievable in the next generation experiments. To invert the left-hand side of the inequality, we solve the equation $3|\langle m_\nu\rangle|^2 - 4|\langle m_\nu\rangle|\sum + (\sum^2 - \delta m^2_{AT}) = 0$. The right-hand side is solved in a similar manner. When $\delta m^2_{AT} \ll \sum^2$, $\delta m^2_{AT} \leqslant 0.005\,\text{eV}$ (99.73% CL), we have

$$|\langle m_\nu\rangle| \leqslant \frac{\sum}{3} \leqslant 2|\langle m_\nu\rangle|. \tag{15}$$

It is evident that next generation neutrinoless double-beta decay experiments are the next important step necessary for a more complete understanding of the physics of neutrinos. In this article we describe several experiments, and discuss ways to evaluate which might reach the desired sensitivity.

1.6. An analytic figure-of-merit for $0\nu\beta\beta$-decay experiments

Any $0\nu\beta\beta$-decay experiment, using presently known technology, will have background. The number of background events, B, can be written:

$$B = bMt\delta E. \tag{16}$$

In equation (16), b is the rate of background counts in $\text{keV}^{-1}\,\text{kg}^{-1}\,\text{year}^{-1}$, M is the source mass in kg, t is the experimental running time in years and δE is the energy window of the $0\nu\beta\beta$-decay events in keV and is proportional to the energy resolution of the detector. In this case, we have assumed as usual that the background under the $0\nu\beta\beta$-peak is approximately constant over the interval δE. In the case that δE is very large, this approximation is less valid because events from $2\nu\beta\beta$-decay can enter the interval δE.

The number of $0\nu\beta\beta$-decay events $C_{\beta\beta}$ can be expressed in terms of the decay rate $\lambda_{\beta\beta}$ as follows:

$$C_{\beta\beta} = \lambda_{\beta\beta}Nt\epsilon = \lambda_{\beta\beta}(A_0 \times 10^3/W)a\epsilon Mt, \tag{17}$$

where A_0 is Avagadro's number, W the molecular weight of the source material, a the isotopic abundance of the parent nuclide and ϵ the detection efficiency of $0\nu\beta\beta$-decay events.

A general criterion for discovery potential for a $0\nu\beta\beta$-decay experiment can be expressed as $C_{\beta\beta} = C_1\sqrt{B + C_{\beta\beta}}$, where C_1 is the confidence level expressed in units of σ of the Poisson distribution. It is convenient to require some specific signal to background ratio, for example $C_{\beta\beta}/B \simeq 1$. In this case, we require $C_{\beta\beta} = \gamma\sqrt{B}$, in which $\gamma = C_1\sqrt{2}$. Although arbitrary this, or any other choice, can be chosen the same for all experiments being compared. Accordingly,

$$\lambda_{\beta\beta}(A_0 \times 10^3)\left(\frac{a\epsilon}{W}\right)Mt = \sqrt{bMt\delta E}, \tag{18}$$

which results in the following expression for the sensitivity:

$$T_{1/2}^{0\gamma} = \alpha \left(\frac{a\epsilon}{W}\right)\sqrt{\frac{Mt}{b\delta E}}. \tag{19}$$

In equation (19), for $C_{\beta\beta} \simeq B$, $\alpha = 7.3 \times 10^{25}$ years. From this relation, a very descriptive expression for a relative figure-of-merit can be derived.

It is more correct to use the total counting rate, $B + C_{\beta\beta}$, in equation (18); however, in cases in which the background is some other multiple of the signal, the result is the same but with a different value of α. If there is no signal, then equation (19) refers to the sensitivity of a bound. If the background is zero, there is no need for equation (19). The factor of α can be chosen the same for all experiments being compared.

Next, we consider the theoretical expression given in equation (4). To account for the theoretical decay rate of the chosen parent isotope we utilize the factor $\overline{\eta} \equiv \langle F_N \rangle \times 10^{13}$, where $\overline{\eta}$ indicates the average of the factor F_N over all nuclear models, and written in shorthand as

$$F_N = G^{0\nu}|M^{0\nu}|^2. \tag{20}$$

A complete figure-of-merit would be proportional to the ratio of the predicted half-life sensitivity appearing in equation (19), and the theoretical half-life for an arbitrary neutrino mass. The latter is proportional to the inverse of the parameter $\overline{\eta}$, so we can simply multiply equation (19) by $\overline{\eta}$. We can eliminate the parameters α and t, which can be chosen the same for all experiments being compared. The resulting expression for the relative figure-of-merit f is then

$$f \equiv \overline{\eta}\left(\frac{a\epsilon}{W}\right)\sqrt{\frac{M}{b\,\delta E}}. \tag{21}$$

From this we see the importance of efficiency and isotopic abundance. They enter the figure-of-merit linearly, while the mass of the source M enters as the square root. This means that to obtain the same increase in half-life sensitivity obtained by doubling the isotopic abundance, the mass would have to be increased by a factor of four, assuming the same background. Of course it is true that the mass M can in principle be continuously expanded, while the parameters 'ϵ' and 'a' are maximum at 1.0. It is also evident that the nuclear structure factor is extremely important, although this is theoretically derived using a nuclear model and has inherent uncertainties. To estimate values of the parameters $\overline{\eta}$ all values from the published literature were used with few exceptions. Values from work that was later determined to be in error was excluded. In addition, values given earlier by the same authors, using the same model were excluded in favour of their later work. Table 4 below lists values of F_N and $\overline{\eta}$ resulting from this averaging process. All other values given in the review by Tretyak and Zdesenko were used [77].

Finally, the energy resolution of the detector is an extremely important characteristic. Foremost, with the excellent energy resolution it is possible to minimize the background produced by the $2\nu\beta\beta$ decay events in the energy window of the 0ν peak. Such a background can only be discriminated from the $0\nu\beta\beta$ decay events, in tracking detectors that have poor energy resolution, however, the better the energy resolution the smaller the contribution of the 2ν tail to the 0ν interval.

Likewise, the role of the energy resolution of the detector is even more crucial for the discovery of the $0\nu\beta\beta$ decay. Since the width of the $0\nu\beta\beta$ decay peak is determined by the energy resolution of the detector, the latter should be sufficient to discriminate this peak from background and to recognize the effect. Practically, it is very useful to determine the minimal level of the

Table 4. Average values of the nuclear structure factors $F_N \equiv G^{0\nu}|M^{0\nu}|^2$, and the corresponding normalized factors $\overline{\eta}$ and $0\nu\beta\beta$-decay energy $|Q_{\beta\beta}|$.

Parent isotope	$\langle F_N \rangle \equiv \langle G^{0\nu}\|M^{0\nu}\|^2 \rangle \text{year}^{-1}$	$\overline{\eta}$	$\|Q_{\beta\beta}\|$ (keV)
^{48}Ca	$(5.4^{+3.0}_{-1.4}) \times 10^{-14}$	0.54	4271
^{76}Ge	$(7.3 \pm 0.6) \times 10^{-14}$	0.73	2039
^{82}Se	$(1.7^{+0.4}_{-0.3}) \times 10^{-13}$	1.70	2995
^{100}Mo	$(5.0 \pm 0.3) \times 10^{-13}$	5.0	3034
^{116}Cd	$(1.3^{+0.7}_{-0.3}) \times 10^{-13}$	1.30	2802
^{130}Te	$(4.2 \pm 0.5) \times 10^{-13}$	4.26	2533
^{136}Xe	$(2.8 \pm 0.4) \times 10^{-14}$	0.28	2479
^{150}Nd	$(5.7^{+1.0}_{-0.7}) \times 10^{-12}$	57.0	3367

energy resolution which is required to detect the $0\nu\beta\beta$ decay with the certain $T^{0\nu}_{1/2}$ value and at a given $2\nu\beta\beta$ decay rate. A quantitative estimate has been made in [84], thus we will follow its definition. With this aim consider figure 2 with three examples, in which the 2ν distribution of ^{116}Cd (with $T^{2\nu}_{1/2} = 3 \times 10^{19}$ years) overlaps the three 0ν peaks with half-lives corresponding to (a) 6.7×10^{23} years; (b) 1.6×10^{25} years; and (c) 3.8×10^{26} years. In figure 2(a) the 0ν peak (with the amplitude M) and $2\nu\beta\beta$ decay spectrum meet at the relative height $h/M = 0.1$, and due to this the separation of the effect is excellent. However, such a demand ($h/M = 0.1$) is very severe. At the same time figure 2(c) demonstrates the other extreme case ($h/M = 1$), which does not allow one to identify the effect at all. The example shown in figure 2(b), where the 2ν distribution and the 0ν peak meet at $h/M = 0.5$, represents the minimal requirement for the observation of the effect, which is still experimentally feasible. Therefore, if we accept the last criterion, the discovery potential of the apparatus with fixed energy resolution can be defined as the half-life of the $0\nu\beta\beta$ decay, which could be measured by satisfying this demand ($h/M = 0.5$) at a given $T^{2\nu}_{1/2}$ value. The dependence of this quantity on the energy resolution was determined for several 2β decay candidate nuclei, and they are depicted in figure 3. We stress that the 'discovery potential' in fact, is the sensitivity for observing the effect and is not the same as the sensitivity to set a limit on the effect searched for. The latter could be much longer than the half-life of the discovery potential.

At this point, we discuss the strategies of several proposed next generation $0\nu\beta\beta$-decay experiments that are designed to achieve the sensitivities to probe much of the range of effective Majorana neutrino mass compatible with neutrino oscillations. Only five are discussed in detail, and 10 others in various stages of development are briefly described.

The ideal $0\nu\beta\beta$-decay experiment has the following dream features: the lowest possible background, the best possible energy resolution, the greatest possible mass of the parent isotope, a detection efficiency near 100% for valid events, a unique signature and the lowest possible construction cost. No single experiment proposed has all of these features. In what follows we discuss in alphabetical order: CUORICINO/CUORE, Enriched Xenon Observatory (EXO), Majorana, Molybdenum Observatory of Neutrinos (MOON) and Neutrino Ettore Majorana Observatory (NEMO). While NEMO-III is by and large a $2\nu\beta\beta$-decay experiment, there is a proposal being developed to enlarge it to be a competitive $0\nu\beta\beta$-decay detector. Later, brief descriptions of the other candidates under consideration will be given.

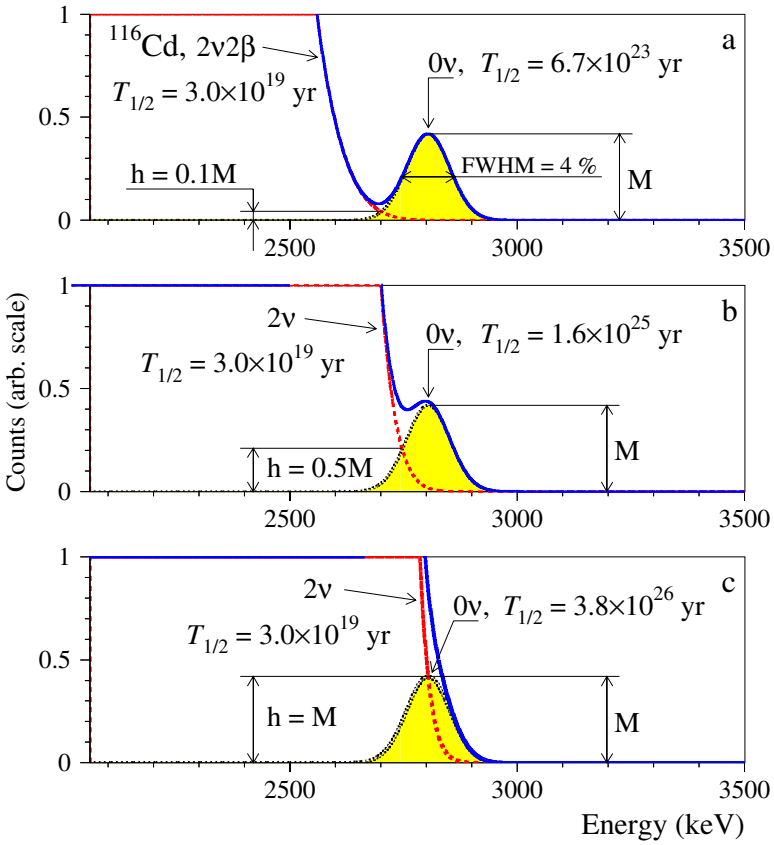

Figure 2. Example of the discovery potential of the 2β decay studies. The 2ν distribution of ^{116}Cd (with $T^{2\nu}_{1/2} = 3 \times 10^{19}$ years) overlaps the 0ν peaks with half-life corresponding to (a) 6.7×10^{23} years; (b) 1.6×10^{25} years; and (c) 3.8×10^{26} years. Correspondingly, the 0ν peak with the amplitude M (the energy resolution at 2.8 MeV is FWHM = 4%) and the 2ν spectrum meet at the relative height h/M for (a) 0.1; (b) 0.5; (c) 1.

Experiments involving Ge detectors or bolometers typically have energy resolutions between 0.2 and 0.3%, and suffer essentially no interference from the irreducible background of events from two-neutrino double-beta decay. Tracking detectors can in principle recognize the difference between neutrinoless and two-neutrino double-beta decay angular correlation; however, angular resolutions of detectors with known technologies are not good enough to eliminate all such events. It is therefore very important to design experiments with the best energy resolution possible for a given detector type. A more quantitative discussion is given at the end of section 4.

2. Next generation experimental proposals

2.1. CUORE/CUORICINO

CUORE is a proposed array of 988 TeO_2 bolometers of about 750 g each. It is best described as a cubic array formed of 19 towers, each similar to the CUORICINO tower which is already

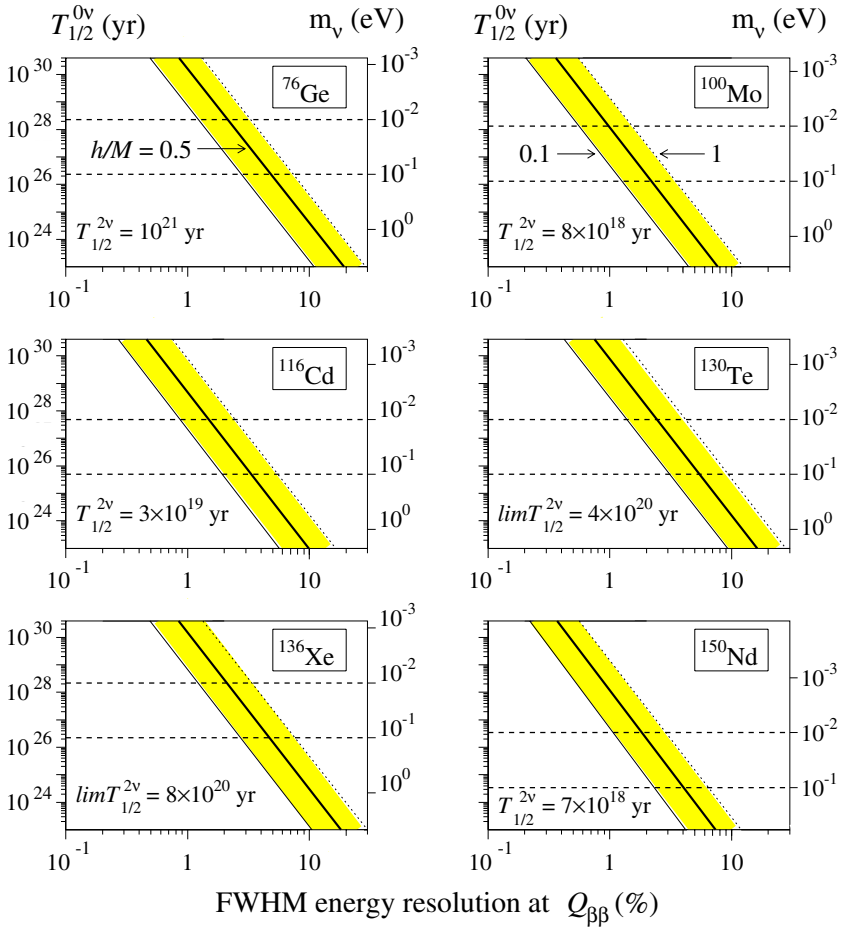

Figure 3. Dependence of the discovery potential versus the energy resolution calculated (bold line for $h/M = 0.5$, thin line for $h/M = 0.1$ and dotted line for $h/M = 1$) for 2β decay candidate nuclei ^{76}Ge, ^{100}Mo, ^{116}Cd, ^{130} Te, ^{136} Xe and ^{150}Nd. Neutrino mass scale (right) is calculated using [75].

operating and producing $0\nu\beta\beta$-decay data as discussed below. All the technical details can be found in the recent CUORE publication by Arnaboldi *et al* [13].

The present CUORICINO array differs slightly from a CUORE tower in that it consists of a tower with 13 planes containing 62 crystals of TeO_2 operating in Hall A of the Gran Sasso Underground Laboratory in the same dilution refrigerator previously used in the MIBETA experiment with 20 crystals [11]. A CUORE tower will have 13 planes of four crystals each. As shown in figure 4, the present CUORICINO structure is as follows: the upper 10 planes and the lowest one consist of four natural crystals of $5 \times 5 \times 5\,\mathrm{cm}^3$, while the 11th and 12th planes have nine, $3 \times 3 \times 6\,\mathrm{cm}^3$ crystals. In the $3 \times 3 \times 6\,\mathrm{cm}^3$ planes the central crystal is fully surrounded by the nearest neighbours.

The small crystals are also of natural tellurium except for four. Two of them are enriched in ^{128}Te and two in ^{130}Te, with isotopic abundances of 82.3 and 75%, respectively. All crystals were grown with pre-tested low radioactivity material by the Shanghai Institute of Ceramics and shipped to Italy by sea to minimize the activation due to cosmic rays. They were lapped with

Figure 4. Photographs of the CUORICINO tower (left), a single plane of four 5 cm cube TeO_2 bolometers (upper right) and one plane of $3 \times 3 \times 6\,cm^3$ bolometers. A CUORE tower will consist of 13 planes of the 5 cm cube bolometers.

specially selected low-contamination abrasives to reduce the radioactive contamination on the surface. All these operations, as well as the mounting of the tower, were carried out in a nitrogen atmosphere glove box in a clean room. The mechanical structure is made of OFHC Copper and Teflon, and both were previously tested for absence of measurable radioactive contaminations. Thermal pulses are recorded by means of neutron transmutation doped (NTD) Ge thermistors thermally coupled to each crystal. The gain of each bolometer is calibrated and stabilized by means of a resistor of 50–100 kΩ, attached to each absorber and acting as a heater. Heat pulses are periodically supplied by a calibrated pulser [7]. The tower is mechanically decoupled from the cryostat to avoid heating due to vibrations, which produce spurious pulses in the detectors. The tower is connected through a 25 mm copper bar to a steel spring fixed to the 50 mK plate of the refrigerator. The entire set-up is shielded with two layers of lead of 10 cm minimum thickness each. The outer layer is made of common low radioactivity lead, the inner layer of special lead with a contamination of 164 Bq kg^{-1} in ^{210}Pb. The electrolytic copper of the refrigerator thermal shields provides an additional shield with a minimum thickness of 2 cm. An external 10 cm layer of borated polyethylene was installed to reduce the background due to environmental neutrons.

The detector is shielded against the intrinsic radioactive contamination of the dilution unit, materials (e.g. from silver and stainless steel) by an internal layer of 10 cm of Roman lead (^{210}Pb activity <4 mBq kg^{-1} [8]), located inside of the cryostat immediately above the tower of the array. The background from the activity in the lateral thermal shields of the dilution refrigerator is reduced by a lateral internal shield of Roman lead that is 1.2 cm thick. It should

be pointed out that in order to use the MIBETA cryostat for the much larger CUORICINO array, the inner thermal shields had to be enlarged. As a consequence the lateral layer of Roman lead was substantially reduced with respect to the configuration of the MIBETA experiment with 20 crystals. The refrigerator is surrounded by a Plexiglas anti-radon box flushed with clean N_2 from a liquid nitrogen evaporator, and by a Faraday cage to eliminate electromagnetic interference.

The front-end electronics of all the $3 \times 3 \times 6\,\mathrm{cm}^3$ detectors and 20 of the 44 detectors of $5 \times 5 \times 5\,\mathrm{cm}^3$ are located at room temperature. They consist of a differential voltage sensitive pre-amplifier followed by a second stage and an anti-aliasing filter [13]. The differential configuration has been adopted to minimize signal cross-talk and microphonic noise coming from the connecting wires. Precautions have been taken to suppress any possible effect coming from room temperature drift and main power supply instability [69]. A pair of load resistors serves to bias each bolometer in a symmetric way. All the necessary settings for the front-end and the biasing system are programmed remotely via computer, to allow the optimization of the overall dynamic performance separately for each detector. The so-called cold electronics have been installed for 24 of the $5 \times 5 \times 5\,\mathrm{cm}^3$ detectors. In this case, the pre-amplifier is located near the detector in a box kept at 100 K to reduce the noise due to microphonics, which is particularly dangerous in the low energy region of the spectrum, relevant for searches for interactions of WIMPS.

The array was cooled down to approximately 8 mK with a temperature spread of 1 mK among the different detectors. A routine calibration was performed using two wires of thoriated tungsten inserted inside the external lead shield in immediate contact with the outer vacuum chamber (OVC) of the dilution refrigerator (see figure 5). This calibration, normally lasting 1–2 days, is performed at the beginning and end of each run, which lasts for approximately 2 weeks.

CUORICINO was cooled down at the beginning of 2003; however, during this operation electrical connections to 12 of the 44 detectors of $5 \times 5 \times 5\,\mathrm{cm}^3$, and to one of the crystals of $3 \times 3 \times 6\,\mathrm{cm}^3$, were lost. This was due to thermal stresses breaking the electrical connection on their thermalizer stages, which allow the transition in temperature in various steps of the electric signals from the detectors to room temperature. When the cause of the technical problem responsible for the disconnection was found, new thermalizer stages were fabricated and tested at low temperature. However, since the performance of the remaining detectors was normal, and their total mass was 30 kg, warming of the array and rewiring were postponed for several months while collecting $0\nu\beta\beta$-decay data.

The performance of the electrically connected detectors was excellent: the average FWHM resolution during the calibration runs was of 7 and 9 keV, for the $5 \times 5 \times 5\,\mathrm{cm}^3$ and the $3 \times 3 \times 6\,\mathrm{cm}^3$ detectors, respectively in the region of $0\nu\beta\beta$-decay.

Double-beta decay measurements started on April 2003 and were interrupted after 3 months due to the disconnection of the cooling water supply of the Laboratory as a consequence of environmental problems associated with the Laboratory itself. During this period CUORICINO operated with a duty factor of 72%, which is very good for a large cryogenic experiment. After the interruption, and a second short run, an independent cooling system was recently installed and CUORICINO is running again.

The first data collection period reported earlier had a total effective exposure of 2.9 and 0.26 kg year for the large and small crystals, respectively. The corresponding spectra in figure 3, show the γ-ray line due to ^{40}K, and those due to the ^{238}U and ^{232}Th chains. Also visible are the lines of ^{121}Te, ^{121M}Te, ^{123M}Te ^{125M}Te and ^{127M}Te, and those of ^{57}Co, ^{58}Co, ^{60}Co, and ^{54}Mn, most likely due to cosmogenic activation of the tellurium and the copper frame. The background counting

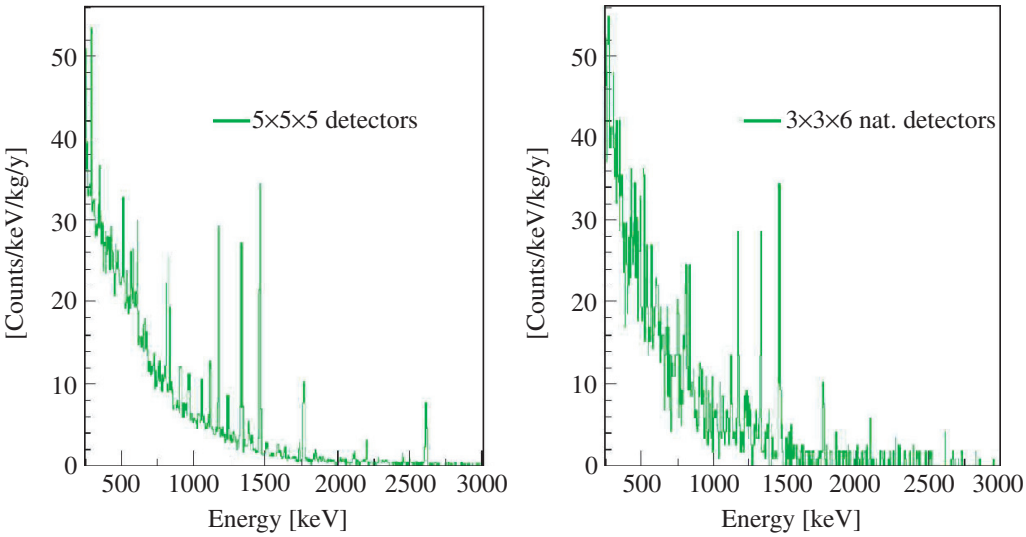

Figure 5. Two calibration spectra of CUORICINO taken with a thorium source shown for the two size detectors.

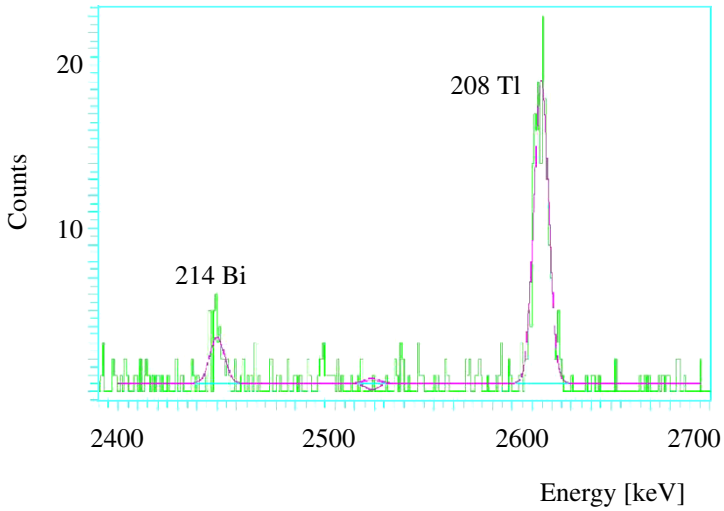

Figure 6. An experimental background spectrum summed over all 5 cm cube detectors. Clearly visible are the two well-known gamma ray lines from the thorium chain, and the energy region of the expected neutrinoless double-beta decay peak.

rates in the region of $0\nu\beta\beta$-decay are 0.20 ± 0.03 and 0.2 ± 0.1 counts keV^{-1} kg^{-1} year^{-1}, for the $5 \times 5 \times 5\,\mathrm{cm}^3$ and $3 \times 3 \times 6\,\mathrm{cm}^3$, respectively. These values are among the best ever obtained in this energy region and similar to those reached in the experiments with Ge diodes [2, 20].

The sum background spectrum of the $5 \times 5 \times 5\,\mathrm{cm}^3$ and $3 \times 3 \times 6\,\mathrm{cm}^3$ crystals is shown in figure 6. No peak appears in the region of $0\nu\beta\beta$-decay of ^{130}Te. A maximum likelihood procedure was used to establish the maximum number of $0\nu\beta\beta$ events. It is consistent with the measured background and implies an upper limit of 7×10^{23} years for $0\nu\beta\beta$-decay of ^{130}Te at a 90% CL. The limits that can be extracted from our result on the effective neutrino mass vary between 0.37

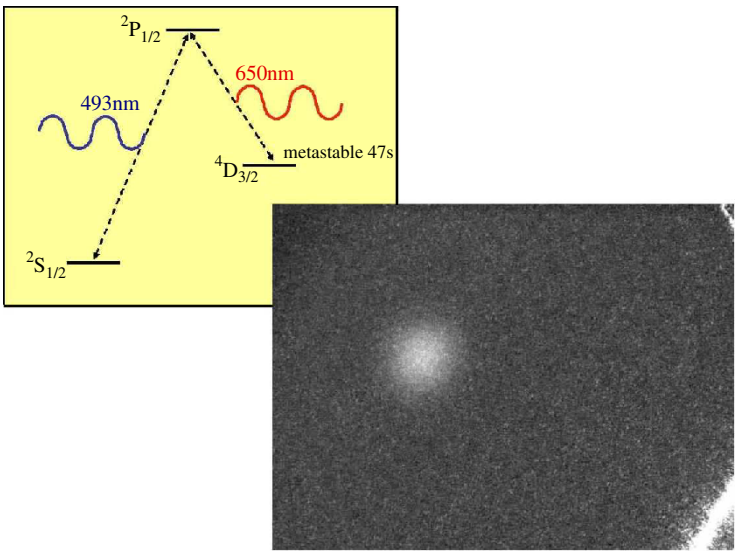

Figure 7. The atomic level scheme for the EXO laser tagging technique, and a photograph of laser light taken in a test chamber.

and 1.9 eV depending on the nuclear matrix elements used. Discussions of the application of matrix elements to arrive at this range are given in the recent paper in *Physics Letters* by the CUORICINO Collaboration [12].

2.2. The EXO experiment

The EXO experiment proposes to search for the $0\nu\beta\beta$-decay of ^{136}Xe to ^{136}Ba in a multi-ton time projection chamber (TPC) of either high-pressure gas or liquid. The decay energy of ^{136}Xe to ^{136}Ba is 2468 keV resulting in a phase-space factor that is competitive with most other candidate isotopes. It has a natural abundance of 8.9% which implies that the Xe must be isotopically enriched. As a noble gas Xe can be enriched by centrifuge with no requirement for complex chemistry, as in the case of all of the other isotopes proposed. A multi-ton detector of enriched ^{136}Xe certainly fulfils the requirement of maximum mass of the parent isotope. While TPCs do not have good energy resolution, there is a research and development program to attempt to tag the daughter $^{136}Ba^{++}$ ion after it is partially neutralized to a more stable $^{136}Ba^{+}$ ion. This was first described by the EXO collaboration in an earlier article by Danilov *et al* [28] from a concept originally introduced by Moe [62].

The scheme involves positively identifying the Ba^+ ion by isolating it and using laser induced fluorescence spectroscopy. The principle of this scheme was first demonstrated by Neuhauser *et al* [65]. The atomic physics can be easily understood from figure 7. The Ba^+ ion has a very strong allowed transition at 493 nm from the $6^2S_{1/2}$ ground state to the $6^2P_{1/2}$ excited state. Upon optical excitation to that state there is a decay branching ratio of 30% to the metastable $5^4D_{3/2}$ state. The specific identification of the Ba^+ ion is achieved by exciting it back up to the $6^2P_{1/2}$ level with photons of 650 nm and observing the 493 nm blue light from the 8 ns 70% transition back to the ground state. When in secular equilibrium, the ion will radiate $\sim 6 \times 10^7$ photons per second. Figure 7 also shows (bottom right) the image of a Ba^+ ion in

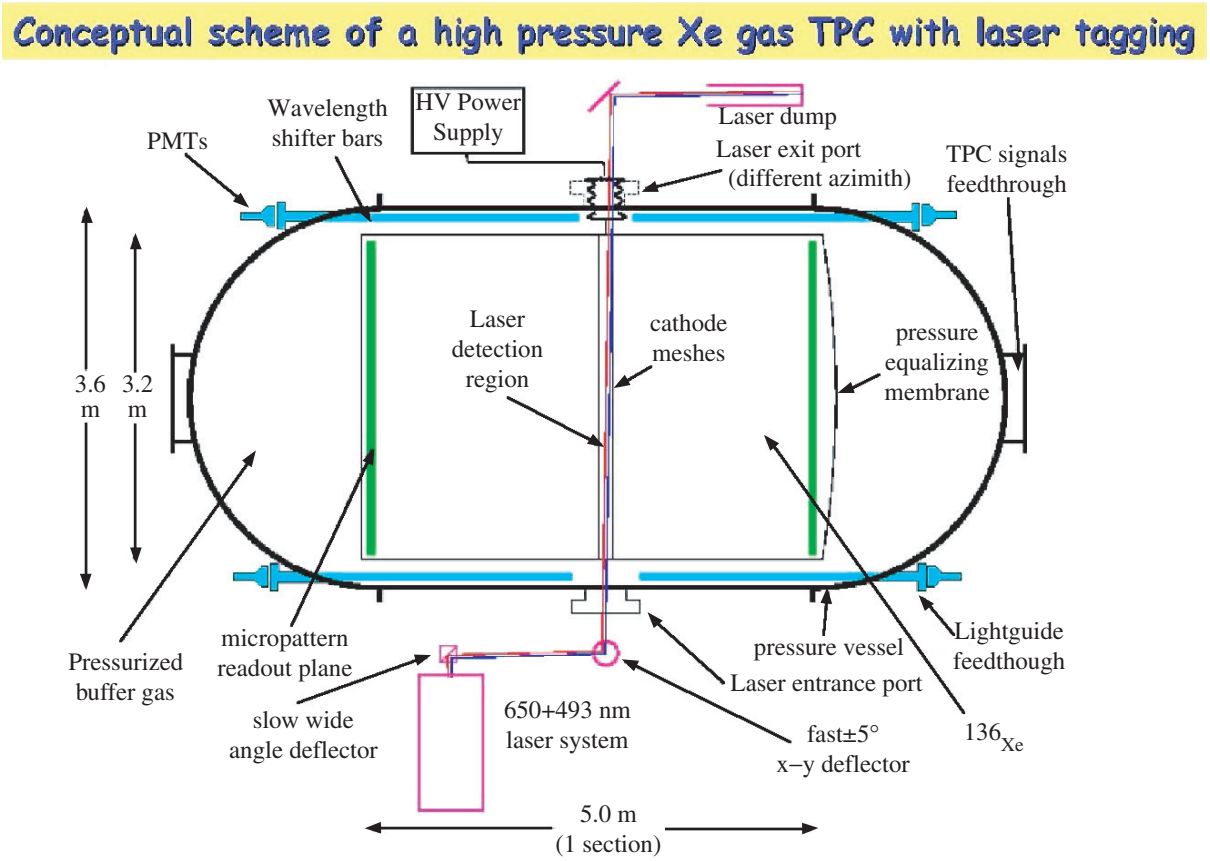

Figure 8. A conceptual drawing of the EXO high-pressure gas TPC, with laser tagging of the Ba^+ ion.

the test trap developed by the EXO group. It will be necessary to hit the ion simultaneously with two laser beams at these two frequencies. The EXO collaboration is at present investigating the spectroscopy of Ba^+ in an atmosphere of Xe at various pressures. In addition, studies are in progress to demonstrate the ability to locate the ion and subject it to the laser excitation and detect the 493 nm light by photo detectors. This principal has been established and repeated many times by the EXO collaboration; however, the main task will be to locate the ion and subject it to the laser excitation and detect the 493 nm light by photomultiplier tubes surrounding the detector.

Several interesting points beyond the principal mechanisms are made in [28]. First, in a gas TPC operated at several atmospheres, the Ba ions will be trapped for a time long enough to localize and excite them. For example, in 5 atmospheres, the Ba ion diffuses only about 0.7 mm in 1 s. In that period of time it can be optically cycled about 10^7 times with the scheme described above. If the drift of the Ba^+ ions in the electric field can be determined accurately, the direction of the laser beams can be corrected. The collaboration has determined that gas pressures of up to 10 atmospheres will also support this detection scheme.

A conceptual drawing of the gas TPC option of EXO is shown in figure 8. A volume of about 40 m^3 of Xe gas at 10 atmospheres would contain about 2 metric tons of xenon. The Xe gas and liquid Xe are also scintillators, and the energy resolution can be improved by detecting both the ionization charge and scintillator light. The collaboration has also been experimenting with a liquid chamber.

The liquid TPC option has the significant advantage of being much smaller than the gas version. The disadvantage of the liquid Xe option is that the laser light will suffer too much scattering to use the technique of locating the Ba^+ ion at the position of the $0\nu\beta\beta$-decay and guiding the lasers to it. The EXO collaboration has been successful in locating Ra ions (very similar to Ba^+ ions) in a small liquid test chamber and extracting it to a small chamber on the tip of a cold-finger electrode coated with frozen Xe. The scheme involves heating the probe and releasing the Ba^+ ion into a radio frequency quadrapole trap, where the laser identification is performed.

Xe is a good scintillator in both gas and liquid phases. This feature will be used to provide a third spatial coordinate in the TPC and improve the energy resolution. This is particularly important for the liquid version of the EXO experiment that is energetically pursued at present. By observing that the scintillation and ionization are anticorrelated, the collaboration has been able to substantially improve the energy resolution such that the resolution in the liquid phase should be able to achieve a resolution of about 2% at 2.5 MeV.

The EXO collaboration is in the process of testing the feasibility of the Ba^+ ion extraction and determining its efficiency. At the same time they have been funded to construct a 200 kg isotopically enriched xenon prototype detector without the Ba^+ ion-tagging feature, and to install and operate it in the DOE Underground Laboratory in the Waste Isolation Pilot Plant (WIPP) in Carlsbad, New Mexico. The results of this pilot experiment could likely be competitive with the most sensitive $0\nu\beta\beta$-decay experiments performed thus far for bounds on the effective Majorana mass of the electron neutrino, providing that reliable nuclear matrix elements are available.

2.3. The Majorana experiment

The proposed Majorana detector is an array of Ge detectors with a total mass of 500 kg of Ge that is isotopically enriched to 86% in ^{76}Ge. The final configuration is not fixed; however, several have been evaluated with respect to cryogenic performance and background reduction and rejection. This discussion will concentrate on a conventional modular design using ultra-low background cryostat technology developed by the International Germanium Experiment (IGEX). It will also utilize new pulse-shape discrimination hardware and software techniques developed by the Majorana collaboration and detector segmentation to reduce background.

The most sensitive $0\nu\beta\beta$-decay experiments thus far have been the Heidelberg–Moscow [20] and IGEX [2, 4] ^{76}Ge projects that set lower limits on $T^{0\nu}_{1/2}$ of 1.9×10^{25} and 1.6×10^{25} years, respectively. They both utilized Ge enriched to 86% in ^{76}Ge and operated deep underground. The projection is that the Majorana background will be reduced by a factor of 65 over the early IGEX results prior to pulse-shape analysis (from 0.2 to $\sim$0.003 $\mathrm{keV^{-1}\,kg^{-1}\,year^{-1}}$). This will occur mainly by the decay of the internal background due to cosmogenic neutron spallation reactions that produce ^{56}Co, ^{58}Co, ^{60}Co, ^{65}Zn and ^{68}Ge in the germanium by limiting the time above ground after crystal growth, careful material selection, and electroforming copper cryostats. One component of the background reduction will arise from the granularity of the detector array. In figure 9, an option for a detector configuration is shown for one module. Each of these modules would have three levels of 19 detectors in close-packed array. Each detector is 62 mm in diameter and 70 mm long with a mass of 1.1 kg. In figure 10, an alternative cooling option is shown which clusters all the detectors in a copper vacuum chamber, which can then be cooled by immersing the chamber in a vessel of liquid nitrogen or in a jacket of cooled gas.

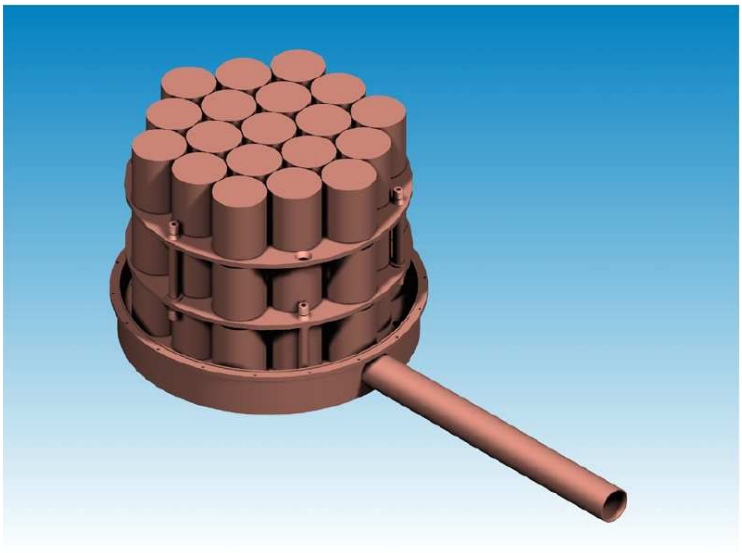

Figure 9. One proposed Majorana module of 57, 1 kg detectors in a standard ultra-low background electroformed copper cryostat.

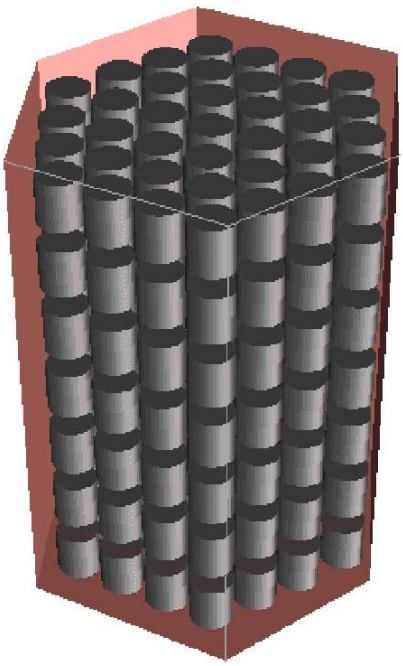

Figure 10. All 259 of the proposed 1 kg Majorana Ge detectors in an alternative cooling configuration.

2.3.1. Recent progress in Ge detector technology. New ^{76}Ge experiments must not simply be a volume expansion of IGEX or Heidelberg–Moscow. They must have superior background rejection and better electronic stability. The summing of 200–250 individual energy spectra can result in serious loss of energy resolution for the overall experiment. In IGEX, instabilities lead to a degradation of 25% in the energy resolution of the 117 mole-years of data.

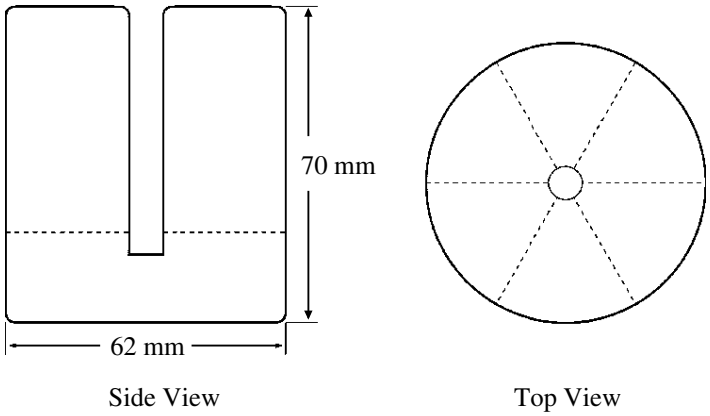

Figure 11. A standard Ge detector segmentation scheme. This is the configuration of the SEGA detector undergoing tests by the Majorana collaboration.

The IGEX collaboration has overcome these problems and the technology is now available. Firstly, detectors electronically segmented into a number of individual volumes in a single n-type intrinsic Ge detector are available from two companies: Advanced Measurement Technology (ORTEC) and Canberra Industries. Secondly, complete digital electronics from X-ray Instrumentation Associates (XIA) have been used by the group to demonstrate unprecedented stability, very low energy thresholds (<1 keV) for a 2 kg Ge detector, and a vast improvement in pulse-shape discrimination.

In the 10 years since the production of the 2 kg IGEX intrinsic Ge detectors, the new technology evolved in the two industrial companies known to us. Large semi-coaxial n-type detectors have been fitted with a series of azimuthal electrical contacts along their length, and one or more axial contacts in the central hole. A configuration with six-azimuthal-segment by two-axial-segment geometry is shown in figure 11. After Monte Carlo studies and discussions with detector manufacturers, several configurations are available that the Majorana collaboration believes will strike a good balance between cost, background reduction and production efficiency. The six-by-two configuration in figure 11 was used in the Monte Carlo simulations that produced the data shown in figure 12 for a single detector. The internal ^{60}Co modelled in the figure is produced by cosmic-ray neutrons during the preparation of the detector. Formation begins after the crystal is pulled. Its elimination by segmentation and pulse shape analysis is crucial.

The saga of pulse-shape discrimination (PSD) in the IGEX project has been slow and painful, finally culminating in success. Current techniques depend entirely on experimental calibration and do not utilize pulse shape libraries. The ability of these techniques to be easily calibrated for individual detectors makes them practical for large detector arrays.

A major contributor to this success has been the availability of commercial digital spectroscopy hardware. Digitizing a detector pre-amplifier signal, all subsequent operations on the signal are performed digitally. Programmable digital filters are capable of producing improved energy resolution, long-term stability and excellent dynamic range. The particular unit used in these studies was the 4-channel Digital Gamma Finder (DGF-4C) unit developed and manufactured by XIA.

The DGF-4C has four independent 14-bit 40 MHz ADCs. The ADCs are followed by first-in first-out (FIFO) buffers capable of storing 1024 ADC values for a single event. In parallel with each FIFO is a programmable digital filter and trigger logic. The digital filter and trigger logic

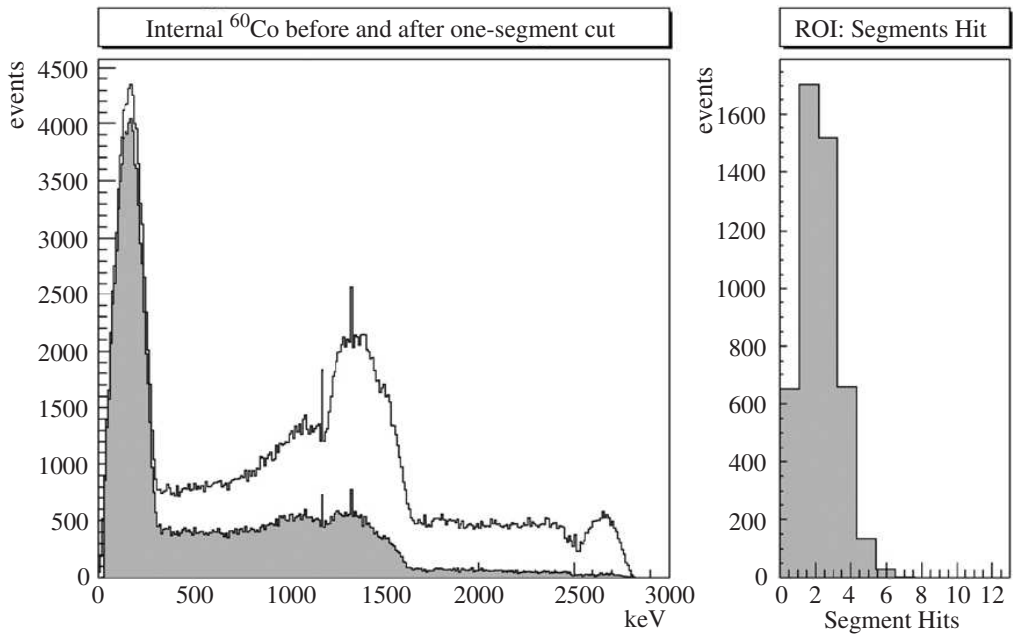

Figure 12. The results of a detailed Monte Carlo simulation of a contamination of ^{60}Co internal to a Ge detector, created by cosmogenic neutrons while the Ge was on the Earth's surface. The upper spectrum is without suppression, and the lower (dark) spectrum is the result of applying cuts that exclude events that interact in more than one segment. The plot to the right is the corresponding frequency plot of events against numbers of segments hit.

for each channel is combined into a single field programmable Gate Array (FPGA). Analog input data are continuously digitized and processed at 40 MHz.

The DGF-4C is then a smart filter of incoming pulses. If for example, a signal has a pulse-width incompatible with the usual collection time of 200–300 ns, or is oscillatory (like microphonic noise), the filters can be programmed to reject it. This feature can also be used to allow the very low energy thresholds required in dark matter searches as well as eliminating the broad spectrum of artificial pulses from high-voltage leaks and electromagnetic interference that can even add noise pulses in the region of $0\nu\beta\beta$-decay. Figure 13 contains two examples of reconstructed pulses from a DGF-4C.

The Majorana Collaboration has made an extensive analysis of the predicted backgrounds and their impact on the final sensitivity of the experiment [60]. Their conclusion is that with 500 kg of Ge, enriched to 86% in the isotope ^{76}Ge, the Majorana array operating over 10 years including construction time, can reach $T^{0\nu}_{1/2} \geqslant 4 \times 10^{27}$ years. This corresponds to an upper bound of $\langle m_\nu \rangle$ of 0.038 ± 0.007 eV [27, 74]. One advantage of ^{76}Ge is that it may well be a candidate for a future more reliable microscopic calculation of the $0\nu\beta\beta$-decay nuclear matrix element.

2.4. MOON

The MOON project involves the use of the unique nuclear structure of the isotope ^{100}Mo for both a neutrinoless double-beta decay search and a solar neutrino experiment [32]. The authors

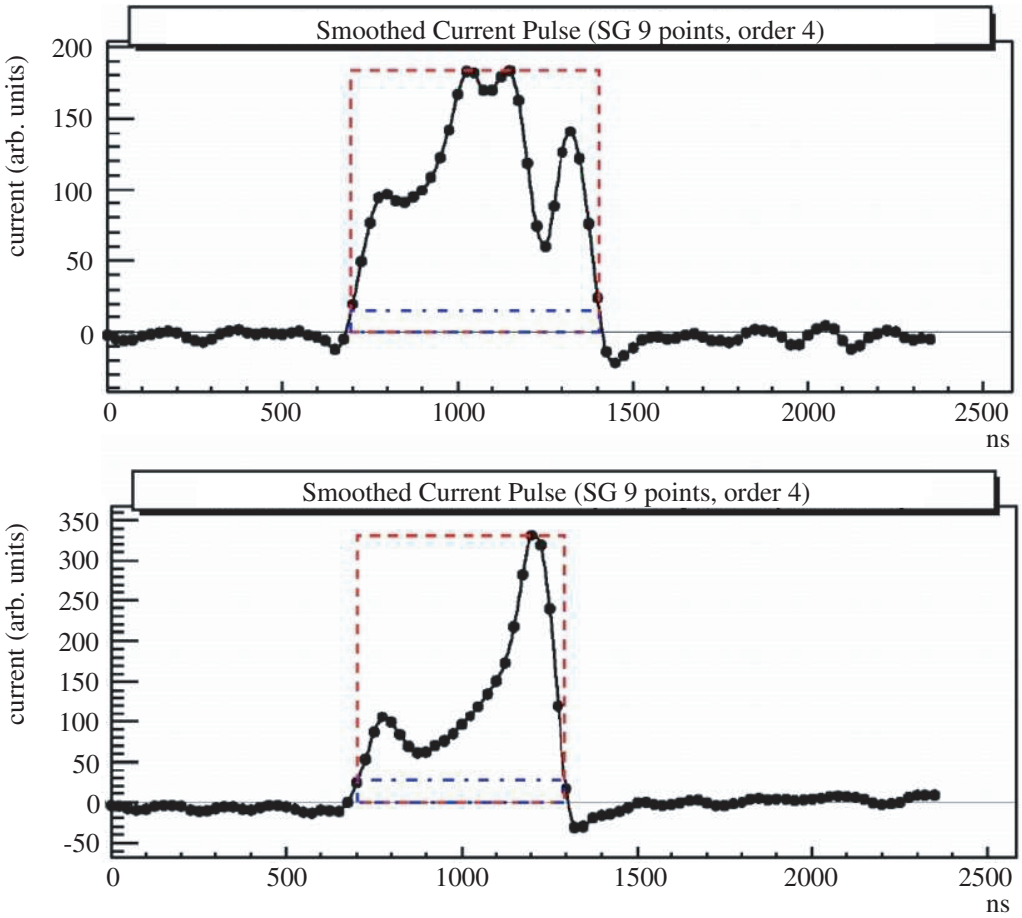

Figure 13. Two typical experimental displacement currents for a multiple-site (upper) curve, like that of a background γ-ray, and (lower) a single-site event like that expected from a neutrinoless double-beta decay event in a Ge detector.

claim that the planned apparatus could also potentially detect supernovae neutrinos [33]. The first excellent feature of ^{100}Mo is that it has a high $0\nu\beta\beta$-decay Q-value, 3034 keV, which results in a large phase space factor in the decay rate, and is above the energies of gamma rays from natural radioactivity as well. The decay of ^{100}Mo has been observed and the half-life accurately measured, most recently by the NEMO Collaboration ($T^{2\nu}_{1/2} = 7.8 \pm 0.09(\text{stat}) \pm 0.09(\text{syst}) \times 10^{18}$) years and discussed later in this article. This short half-life unfortunately has the potential effect of contributing a non-reducible background from $2\nu\beta\beta$-decay to the energy region of $0\nu\beta\beta$-decay. This implies that significant attention must be paid to achieving the best possible energy resolution near the $0\nu\beta\beta$-decay energy, 3034 keV.

The basic detector concept involves constructing a tracking chamber of series of planes of thin films of Mo sandwiched between plastic scintillating fibres. The fibres on one side would be perpendicular to those on the other side of the Mo foils. Each sandwich is followed by a 6 mm thick plastic scintillator to obtain the energy of the electrons. This configuration, shown in figures 14 and 15, is designed to track decay electrons well enough to observe the angular correlation of pairs of electrons from the source to reject background from $2\nu\beta\beta$-decay, as well as some others. Another concept under consideration is the use of plastic scintillating fibres coated

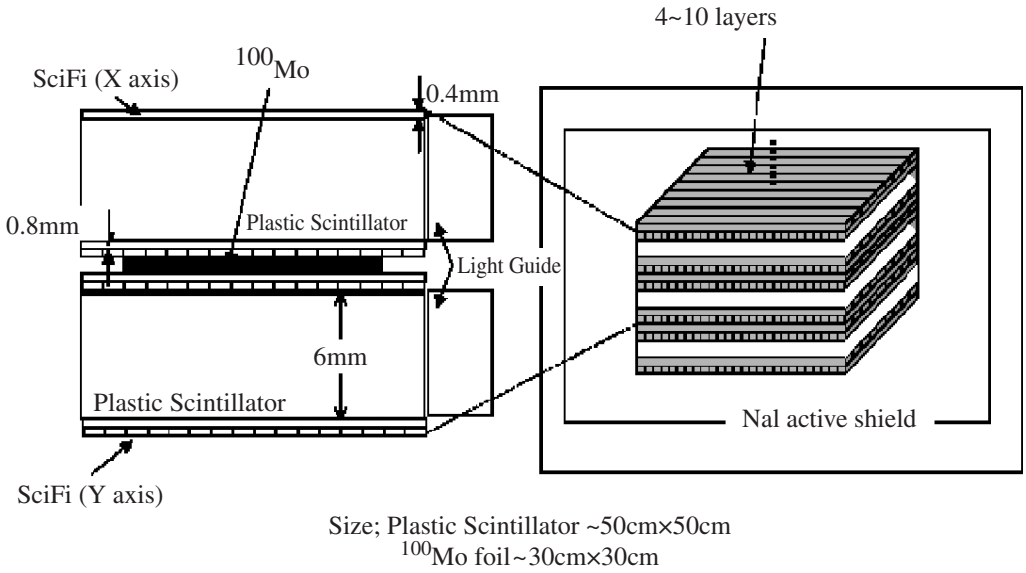

Figure 14. An artist's conception of a module of the MOON detector showing the ^{100}Mo foil, readout fibres, and the plastic scintillators.

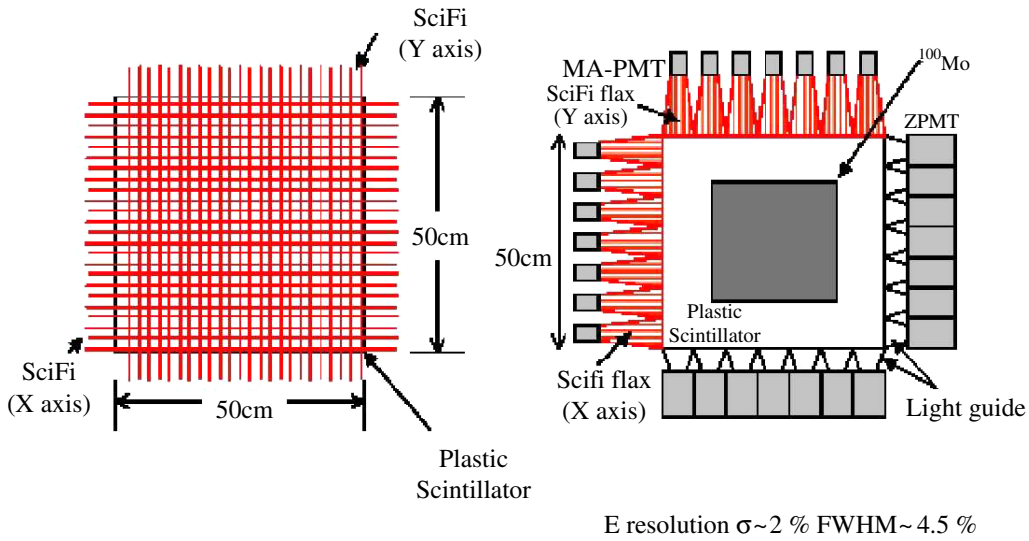

Figure 15. The configuration for testing the energy resolution of the MOON modules. The tests yielded a resolution of FWHM = 4.5% at the double-beta decay energy of ^{100}Mo.

with about 0.03 g cm^{-2} of Mo. This geometry could achieve a position resolution of the order of the fibre diameter, which is typically 1–3 mm. The signal characteristic of double beta-decay in the MOON detector is a coincidence between two beta particles in two independent parts of the detector. This will help to reduce backgrounds. This, coupled with the angular correlation, can combine to lead to significant background reduction. This is of crucial importance because in building a tracking detector it is far more difficult to control the radio-purity of all of the constituent components than in the case of Ge detectors, for example. The predicted $0\nu\beta\beta$-decay

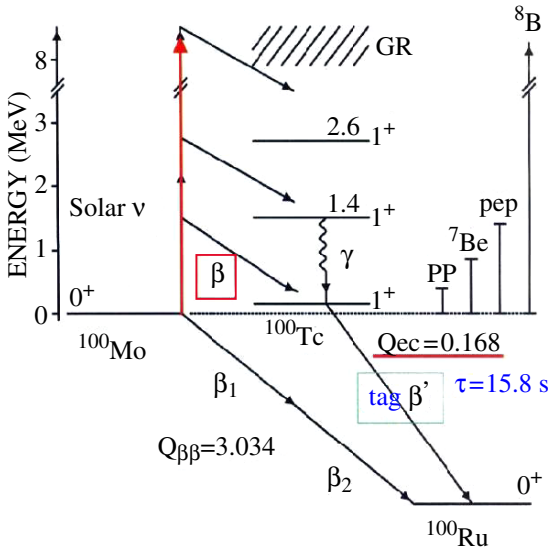

Figure 16. The nuclear decay-scheme of ^{100}Mo, demonstrating its value as a solar neutrino detector as well as a source for neutrinoless double-beta decay.

rate for the target sensitivity, $\langle m_\nu \rangle = 0.03$ eV, is ~11 counts ton^{-1} year^{-1} of enriched ^{100}Mo. The natural abundance is 9.63%.

The very special nuclear structure of the three isotopes, ^{100}Mo, ^{100}Tc and ^{100}Ru are shown in figure 16. This energy level scheme renders ^{100}Mo a good target for the study of low-energy solar neutrinos as well as an excellent candidate for the search for neutrinoless double-beta decay. There is need for a low energy, real-time spectroscopy study of solar neutrinos. The low excitation energy from the ground state of ^{100}Mo to the low-lying 1^+ state, with an electron-capture Q-value of 168 keV, decays to the ground state of ^{100}Ru with a half-life of 15.8 s. This transition would be sensitive to pp-neutrinos as well as ^{7}Be and pep neutrinos. The ^{8}B solar neutrinos would excite higher energy 1^+ states in ^{100}Tc which would decay by gamma-ray cascade to the low-lying 1^+ state that decays by β^- to the ground state of ^{100}Ru with the half-life of 15.8 s.

Energy resolution tests are underway with a $60 \times 60 \times 10\,\text{mm}^3$ plate with four 2 in photomultiplier tubes at right angles. A resolution of $\sigma = 2.7\%/E^{1/2}$ has been achieved. For the full MOON modules, a resolution of FWHM = 5% is predicted at the $0\nu\beta\beta$-decay energy of 3034 keV. The two tracking measurements, together with the signal selection by the time and spatial correlation analyses, reduces most background counts from natural and cosmogenic radio isotopes and $2\nu\beta\beta$-decay. The MOON-decay experiment is planned in three phases: MOON-I, 0.003 ton year, MOON-II, 0.75 ton year and MOON-III, 5.25 ton year. The predicted half-life sensitivities are: 6×10^{25}, 8×10^{26} and 3×10^{27} years, respectively. The corresponding upper bounds on the effective Majorana mass of the electron neutrino $\langle m_\nu \rangle$ are 0.1, 0.03 and 0.02 eV, respectively.

The large area of foils could lead to significant difficulties in controlling the background from radon daughters and dust; however, this could be significantly alleviated by the use of Mo foils isotopically enriched in ^{100}Mo. This has been accomplished several times at the Electro-Chemical Plant in Zelenogorsk (Russia) by use of centrifuge separation using MoF_6 gas.

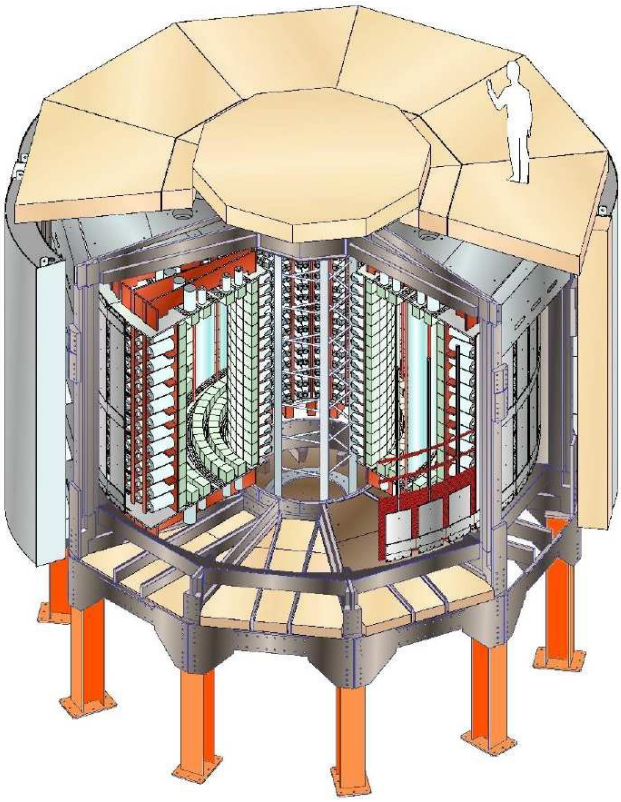

Figure 17. An artist's conception of the NEMO detector, showing a cartoon of a normal size person to demonstrate its dimensions.

2.5. Nemo and Super-NEMO

The NEMO has had several generations. Here, we describe NEMO-3, which is operating, and give projections for an expanded version that would represent a next generation $0\nu\beta\beta$-decay experiment. In this paper, we have emphasized both source = detector calorimeter experiments, CUORE, and Majorana, and two types of tracking detector experiments, a TPC in which the source is also the detector namely EXO, and finally two types of tracking chambers, MOON, and finally now NEMO [15].

The NEMO-3 detector is constructed in 20 segments of thin source planes, a three-dimensional readout drift chamber, operating in the Geiger mode for tracking, with the tracking volumes surrounded by plastic scintillating blocks as calorimeters. There are 1940 plastic scintillators that have thresholds of ∼30 keV and a γ-ray detection efficiency of 50% at 1 MeV. At this energy, the energy resolution ranges between 11 and 14.5% FWHM. The planes are vertically set in a cylindrical geometry inside of a magnetic solenoid that creates a vertical induction field of ∼30 G. Tracking in the field allows the differentiation between electron and positron tracks, with only a probability of ∼3% of confusing the two. Figure 17 shows a schematic drawing, while figure 18 is a photograph of the open detector.

The detector is surrounded by a 20 cm shield of low background iron to reduce the external gamma ray flux. Fast neutrons from the laboratory environment are suppressed by an external shield of water, wood and polyethylene plates. The experiment is located in the Modane

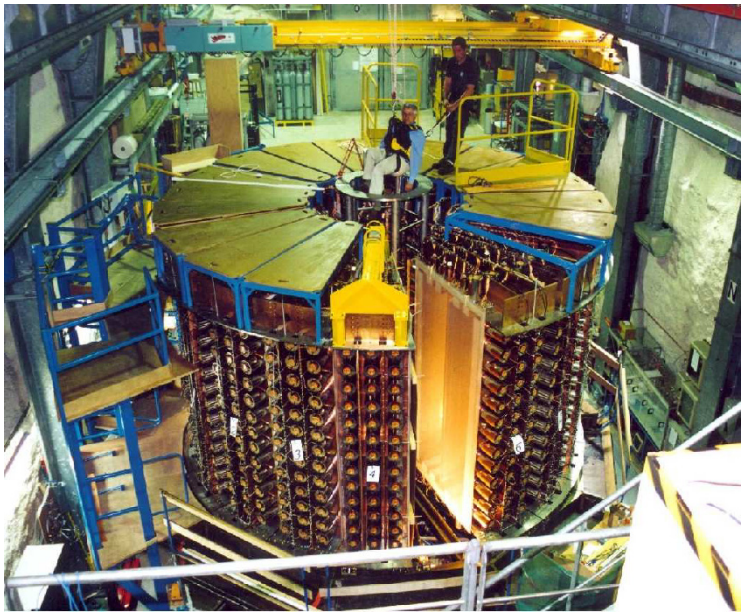

Figure 18. A photograph of the NEMO detector opened and showing one of its source foils. Note the people on top of the detector.

Underground Laboratory with an overburden of 4800 m of water equivalent (mwe). The air in the experimental hall is constantly flushed which reduces the radon levels to between 10 and 20 Bq m^{-3}. This renders the number of decays of ^{214}Bi in the detector due to radon to be below that due to the photomultiplier tubes. This level was further reduced by the installation of a tent surrounding the detector which during this year will have its atmosphere purified by a Free-Radon Purification System to reduce radon levels to ∼0.2 Bq m^{-3}, with a capacity of 150 m^3 h^{-1}.

One very positive aspect of the NEMO detector is that it can make double beta-decay measurements on many different nuclei, and several simultaneously. During recent operations the following isotopes were together investigated in the detector: ^{116}Cd (0.40 kg),^{130}Te (0.45 kg), ^{150}Nd (36.5 g), ^{96}Zr (9.43 g), ^{48}Ca (6.99 g), ^{nat}Te (0.61 kg), ^{82}Se (0.93 kg) and ^{100}Mo (6.9 kg). Two neutrino double beta-decay half-lives were measured and the following three results were communicated to us at the time of the Venice conference in December 2003:

$$T^{2\nu}_{1/2}(^{150}\mathrm{Nd}) = 7.5 \pm 0.3(\mathrm{stat}) \pm 0.7(\mathrm{syst}) \times 10^{18}\mathrm{years}, \tag{22}$$

$$T^{2\nu}_{1/2}(^{82}\mathrm{Se}) = 9.52 \pm 0.25(\mathrm{stat}) \pm 0.9(\mathrm{syst}) \times 10^{19}\mathrm{years}, \tag{23}$$

and

$$T^{2\nu}_{1/2}(^{100}\mathrm{Mo}) = 7.8 \pm 0.09(\mathrm{stat}) \pm 0.09(\mathrm{syst}) \times 10^{18}\mathrm{years}. \tag{24}$$

The two-electron sum spectrum from the $2\nu\beta\beta$-decay of ^{100}Mo is shown in figure 19. This is essentially a zero background spectrum, and is the highest quality one ever published to the knowledge of the authors of this review. One of the reasons for this is that backgrounds from the usual problem sources, ^{214}Bi and ^{208}Tl for example can be recognized by their known decay chains and the life times of their daughter nuclides, and identified.

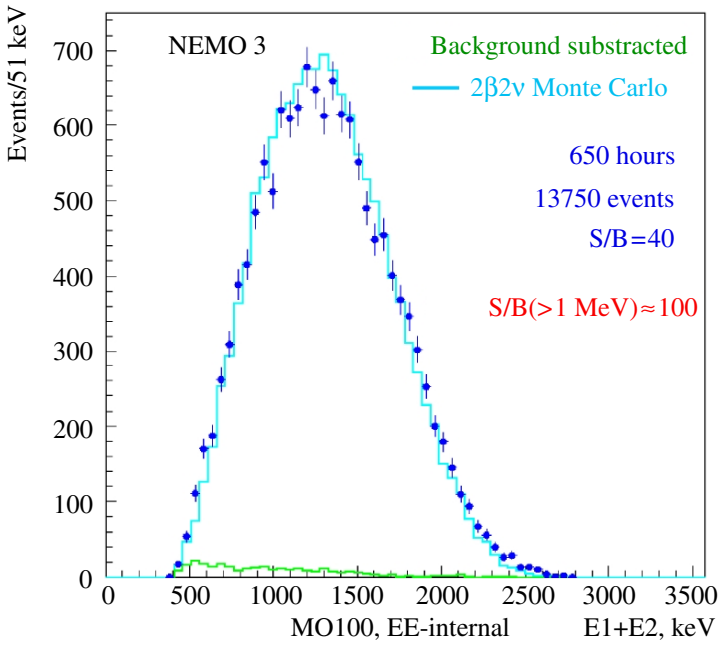

Figure 19. An energy spectrum of the sum energy of the two electrons from the two-neutrino double-beta decay of ^{100}Mo measured in the NEMO detector.

The remaining challenge concerns the energy resolution, which in NEMO-3 is about 250 keV at 3 MeV. This will require a convincing discovery experiment to have enough real counts from $0\nu\beta\beta$-decay in order to determine that a peak really exists. Nevertheless, the series of NEMO experiments have really made significant contributions to the field of double-beta decay and the technique has some promise for the future. Discussions are in progress to consider a greatly expanded version, SuperNEMO, as a next generation $0\nu\beta\beta$-decay experiment.

The basic parameters for SuperNEMO are that they be at least ten times the capacity of NEMO-3 so that it will have the capacity to contain about 100 kg of isotopically enriched isotope. Candidate isotopes are ^{82}Se, ^{100}Mo, ^{116}Cd, ^{130}Te and ^{136}Xe.

The project is conceived to have four phases: (i) (2004–2006), feasibility studies, (ii) (mid 2006–2007) engineering design and acceptance, (iii) (2008–2010) construction; and (iv) (2011–) operation.

One of the main issues in feasibility study is the attempt to improve the energy resolution. The requirement for a significant breakthrough here will quite possibly be the driving force for full proposal.

3. Other proposals

There are other proposals that merit some discussion. These proposals can be divided into two categories, those with an active source and those with a passive source. Active source experiments use detectors that are fabricated from the source material and passive source detectors use separate sources and detectors. The following are descriptions of other experiments not covered earlier in this article.

Table 5. Physical properties of $CaWO_4$ and $CdWO_4$ crystal scintillators.

Physical parameter	$CaWO_4$	$CdWO_4$
Density (g/cm^3)	6.1	8.0
Melting point (°C)	1570–1650	1325
Structural type	Sheelite	Wolframite
Cleavage plane	(1 0 1)	(0 1 0)
Hardness (Mohs)	4.5–5.0	4.0–4.5
Wavelength of emission maximum (nm)	440	480
Refractive index	1.94	2.2–2.3
Primary decay time	8 μs	13 μs
Relative light yield (for γ-rays, at indoor temperature)	≈90%	100%

3.1. CARVEL: an example of a scintillator double-beta decay experiment

The CAlcium Research for VEry Low neutrino mass (CARVEL) experiment is being developed using scintillator crystals of $^{48}CaWO_4$ [83]. A research project performed by the Institute for Nuclear Research (Kiev, Ukraine) has verified the ability of these crystals to discriminate between pulses from α-particles and electrons. There was a rather high level of radioactivity in the $CaWO_4$ crystals used in the development; nevertheless a background level of 0.07 counts $kev^{-1}\,kg^{-1}\,year^{-1}$ was achieved in the energy region of $0\nu\beta\beta$-decay. The high decay energy, 4272 keV, of ^{48}Ca is well above the natural radioactivity level of gamma rays. In principle, 100 kg of $^{48}CaWO_4$ could reach a sensitivity of $m_\nu \simeq 40$–90 meV or $T^{0\nu}_{1/2} \sim 10^{27}$ years. One ton could reach $T^{0\nu}_{1/2} \sim 10^{28}$ years and $m_\nu \sim 20$ meV.

The difficulty of immediately proposing such an experiment at this time stems from the fact that the only known practical method for isotopically enriching Ca in ^{48}Ca in kg quantities is the atomic vapor laser ionization separation (AVLIS) technique. The cost is roughly proportional to the ratio of the final isotopic abundance to the initial one, which is only 0.187%. The atomic structure of calcium however has favourable laser wavelength requirements, and is called a 'first harmonic candidate'. The only facility to our knowledge in existence at the time of writing this paper is at the Lawrence Livermore National Laboratory, Livermore, CA, USA. This facility does not have a program for enriching large quantities of isotopes at the moment. There is a program of development at the Kurchatov Institute (Moscow), which could possibly lead to a practical solution in the future.

In table 5, the properties of $CaWO_4$ and $CdWO_4$ are given. They have very similar light output, however, earlier experiments demonstrated that the radioactive background achieved in the $CdWO_4$ crystals was much lower than that of the $CaWO_4$ scintillator. This strongly implies that the background in the $CaWO_4$ can quite probably be reduced significantly.

The scintillation properties of $CaWO_4$ crystal scintillators were studied. The energy resolution of $CaWO_4$ detectors is similar to that of NaI(TI) scintillators (e.g., FWHM ≈ 7% for the 662 keV γ line of ^{137}Cs and FWHM = 3.8% for the 2614 keV γ line of ^{208}TI). Due to the difference of $CaWO_4$ scintillation pulse shapes for α particles and γ-rays (β particles), clear discrimination between them was achieved. Radioactive contaminations of the $CaWO_4$ crystals are higher by factors from 10 to 10^3 (e.g., activity of ^{210}Po is ≈0.3 Bq kg^{-1}) than those of the $CdWO_4$ scintillators.

3.1.1. Pulse shape discrimination in scintillation detectors. The pulse shape of $CaWO_4$ scintillation signals, for example, can be described by the formula: $f(t) = \sum A_i/(\tau_i - \tau_0) \times (e^{-t/\tau_i} - e^{-t/\tau_0})$, $t > 0$, where A_i are amplitudes (in %) and τ_i are decay constants for different light-emission components, τ_0 is the integration constant of electronics ($\approx$0.2 μs). The following values were obtained by fitting the average of 4000 individual pulses: $A_1^\alpha = 0.76$ $\tau_1^\alpha = 8.8\,\mu$s, $A_2^\alpha = 0.18$, $\tau_2^\alpha = 3.2\,\mu$s, $A_3^\alpha = 0.06$, $\tau_3^\alpha = 0.3\,\mu$s, for $\approx$4.6 MeV α particles and $A_1^\gamma = 0.82$, $\tau_1^\gamma = 9.0\,\mu$s, $A_2^\gamma = 0.15$, $\tau_2^\gamma = 4.4\,\mu$s, $A_3^\gamma = 0.03$, $\tau_3^\gamma = 0.3\,\mu$s, for $\approx$1 MeV γ quanta. This difference allows one to discriminate $\gamma(\beta)$ events from those of α particles. For this purpose, the method of the optimal digital filter, previously applied successfully with $CdWO_4$ scintillators, was used. To obtain the numerical characteristic of $CaWO_4$ signals, called the shape indicator (SI), each experimental pulse $f(t)$ was processed with the following digital filter: $SI = \sum f(t_k) \times P(t_k)/\sum f(t_k)$, were the sum is over time channels k, starting from the origin of the pulse and up to 75 μs, $f(t_k)$ in the digitized amplitude (at the time t_k) of a given signal. The weight function P(t) is defined as $P(t) = \{\bar{f}_\alpha(t) - \bar{f}_\gamma(t)\}/\{\bar{f}_\alpha(t) + \bar{f}_\gamma(t)\}$, where $\bar{f}_\alpha(t)$ and $\bar{f}_\gamma(t)$ are the reference pulse shapes for α particles and γ quanta, resulting from the average of a large number of experimental pulse shapes.

The shape indicator measured by $CaWO_4$ crystals for α particles in the (1–5.3) MeV region does not depend on the direction of α irradiation relative to the crystal axes. Similarly, no dependence of the SI on γ quanta energy (from 0.1 to 2.6 MeV) was observed. The distributions of the shape indicators measured with α particles ($E_\alpha \approx 5.3$ MeV) and γ quanta ($\approx$1.2 MeV) are depicted in the inset of figure 20 (the larger value of the shape indicator corresponds to the shorter decay time of the scintillation pulse). As shown in figure 20, distinct discrimination between α particles and γ rays (β particles) was achieved. As an illustration of the PS analysis, the background data, accumulated during 171 h with $CaWO_4$ detector, is shown in figure 19 as a scatter plot for the SI values versus energy. In this plot one can see two clearly separated populations: the α events, which belong to U/Th families and $\gamma(\beta)$ events.

In figure 21, the effect of the energy resolution projected to 4272 keV on the interference from $2\nu\beta\beta$-decay is shown.

The CARVEL project has produced some interesting data associated with the properties of $CaWO_4$ and $CdWO_4$ crystal scintillators. They have the light output that results in adequate energy resolution. Pulse-shape analysis leads to clear discrimination between α-particle and γ-ray induced events allowing significant background reduction. Future availability of Ca, isotopically enriched in ^{48}Ca could render this technique competitive. These results could be interesting for the investigation of other double beta-decay scintillation detectors.

3.2. The ^{116}Cd CAMEO project

The project CAMEO [21] is a further development of the double beta-decay studies of ^{116}Cd performed by the Kiev–Florence collaboration in the Solotvina Underground Laboratory since 1989 with enriched cadmium tungstate ($^{116}CdWO_4$) crystal scintillators [29, 31]. Here, we briefly describe the main results of this experiment. $^{116}CdWO_4$ scintillators (enriched in ^{116}Cd to 83%) with a total mass of 330 g were used. They were surrounded by active and passive shields. For each event in the $^{116}CdWO_4$ detector, the amplitude of the signal, its arrival time and pulse-shape were recorded. The energy resolution of the detector was FWHM = 8.0% at 2615 keV. Due to active and passive shields, and as a result of the time-amplitude and pulse-shape analysis of the data, the background rate of the $^{116}CdWO_4$ detector in the energy interval 2.5–3.2 MeV ($Q_{\beta\beta}$

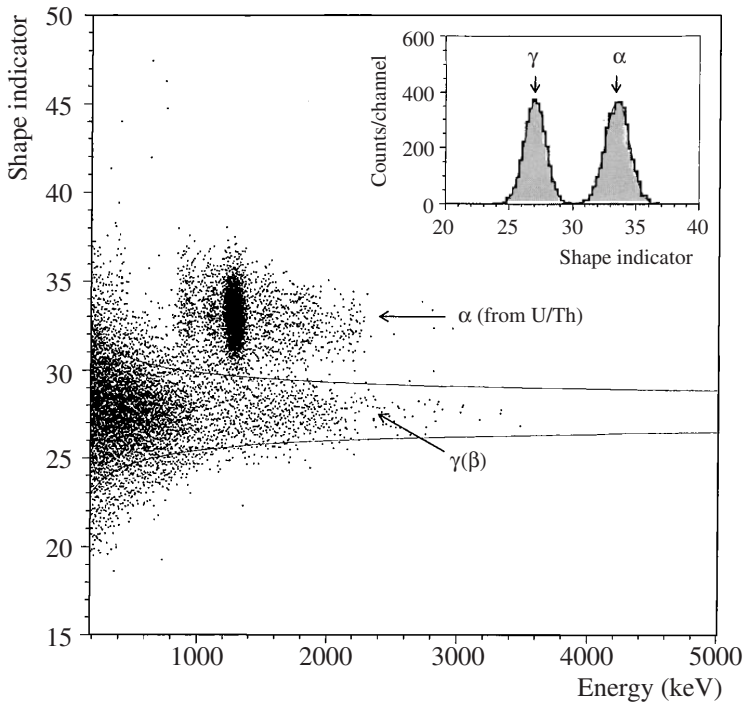

Figure 20. Scatter plot of the shape indicator SI versus energy for 171 h background data measured with the $CaWO_4$ crystal scintillator ($40 \times 34 \times 23\,mm^3$). The solid liner show $\pm 2\delta$ region of SI for $\gamma(\beta)$ events. Inset: the SI distributions measured in calibration runs with α particles ($E_\alpha = 5.3$ MeV) which corresponds to $\approx$1.2 MeV in γ scale and γ quanta ($\approx$1.2 MeV).

of ^{116}Cd is 2.8 MeV) was reduced to 0.037(10) counts year^{-1} kg^{-1} keV^{-1}. This is the lowest background rate which has ever been reached with crystal scintillators.

A fit of the data measured during 12649 h gives the half-life value of the $2\nu\beta\beta$ decay of ^{116}Cd:

$$T^{2\nu}_{1/2} = 2.9 \pm 0.06(\text{stat})^{+0.4}_{-0.3}(\text{syst}) \times 10^{19}\ \text{years}.$$

In addition, the bound on the half-life for $0\nu\beta\beta$-decay of ^{116}Cd was measured as

$$T^{0\nu}_{1/2} \geqslant 1.7(2.6) \times 10^{23}\ \text{yr at } 90\%(68\%)\text{CL}.$$

Using this limit and the calculations of [75], one can derive restrictions on the neutrino mass parameter $\langle m_\nu \rangle \leqslant 1.7(1.4)$ eV at 90% (68%) CL, or on the basis of calculations [14] $\langle m_\nu \rangle \leqslant 1.5(1.2)$ eV.

These bounds, which are among the best published to date, were obtained with very small $^{116}CdWO_4$ detectors (containing only $\approx$0.1 kg of ^{116}Cd, in contrast with those used for ^{76}Ge studies ($\approx$10 kg of enriched HP ^{76}Ge detectors). Therefore, the Solotvina experiment demonstrates that $CdWO_4$ crystals possess several unique properties required for a double beta-decay experiment: low-level intrinsic radioactivity, good scintillation characteristics and PSD ability, which allows one to reduce background. To enhance the sensitivity to $\langle m_\nu \rangle \leqslant 0.05$ eV,

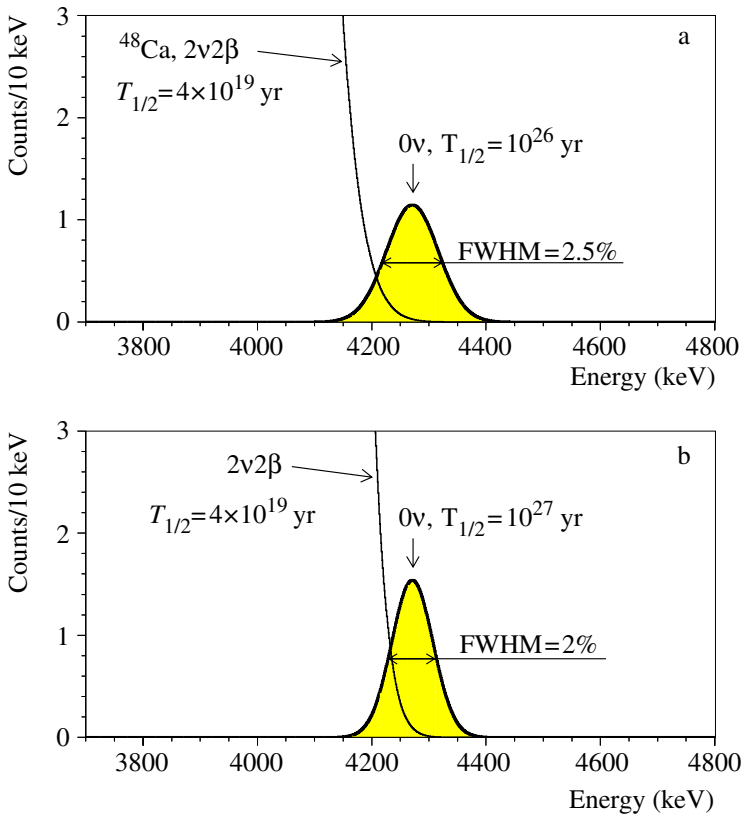

Figure 21. A demonstration of the impact of energy resolution of $|Q_{\beta\beta}|$ on the interference from $2\nu\beta\beta$-decay events.

it will be necessary to increase the mass of enriched $^{116}CdWO_4$ detector and measuring time, to improve the energy resolution and to reduce the background of the detector further.

Accordingly, the CAMEO project [21] proposes to use ≈100 kg of $^{116}CdWO_4$ crystals placed in a large volume of high purity liquid (serving as a shield and a light guide simultaneously), and calls for improvement of the energy resolution (FWHM) at 2.8 MeV to 4%, and for the background reduction by a factor ≈100. The required radioactive contamination of $^{116}CdWO_4$ crystals must be less than ≈10 μBq kg^{-1}, both for ^{228}Th and ^{226}Ra. Actually, even existing $CdWO_4$ crystals satisfy these requirements for ^{226}Ra (<4 μBq kg^{-1}), but ^{228}Th contamination varies in different crystals from (3–39) μBq kg^{-1} [31]. At the same time, the required energy resolution FWHM = 4.3% at 2615 keV (^{232}Th) has been already achieved with the $CdWO_4$ crystal ($\oslash 4 \times 3$ cm^3) placed in a liquid.

In the preliminary design concept of CAMEO, 24 enriched $^{116}CdWO_4$ crystals of large volume (≈350 cm^3) are allocated for the liquid scintillator of the BOREXINO Counting Test Facility (CTF)[2] and fixed at 0.4 m distance from the CTF centre, thus homogeneously spreading

[2] The CTF (described, e.g., in [9] is installed in the Gran Sasso Underground Laboratory (Italy). It consists of an external ≈1000 ton water tank (11 × 10 m) served as passive shield for 4.8 m^3 liquid scintillator (contained in an inner vessel of diameter 2.1 m). The radio-purity of the water is ≈10^{-14} g g^{-1} for U/Th and ≈10^{-10} g g^{-1} for K. The liquid scintillator is a solution of 1.5 g l^{-1} of PPO in pseudocumene. The yield of emitted photons (365 nm) is ≈10^4 MeV^{-1} and the attenuation length is ⩾5 m. The principal scintillator decay time is ≈5 ns. The ^{232}Th and

on the sphere with diameter 0.8 m. On the basis of GEANT Monte Carlo simulations, the sensitivity of the CAMEO experiment has been calculated as $T^{0\nu}_{1/2} \geqslant 10^{26}$ years, which translates to the neutrino mass parameter bound of $\langle m_\nu \rangle \leqslant 0.06$ eV. Moreover, these results can be advanced further by exploiting 1 ton of $^{116}CdWO_4$ detectors ($\approx 1.5 \times 10^{27}$ nuclei of ^{116}Cd) placed in one of existing or future large underground neutrino detectors such as BOREXINO, SNO or KamLAND. The sensitivity is estimated as $T^{0\nu}_{1/2} \geqslant 10^{27}$ years ($\langle m_\nu \rangle \leqslant 0.02$ eV). The proposed CAMEO technique with $^{116}CdWO_4$ crystals is simple and reliable, thus, such experiments can run stably for decades.

For isotopic enrichment, a new project, MCIRI, is under development at the Kurchatov Institute (Moscow), and the Joint Institute for Nuclear Research (Dubna), with the goal to enrich large quantities of ^{48}Ca (and other isotopes) by ion cyclotron resonance heating in plasma [40]. This could certainly enhance interest in $0\nu\beta\beta$-decay experiments using ^{48}Ca.

3.3. Double-beta decay of ^{48}Ca with CANDLES

The CANDLES project is a search for $0\nu\beta\beta$-decay of ^{48}Ca with scintillators of CaF_2 (pure) immersed in liquid scintillator. It will be installed in the underground Oto Cosmo Observatory. The original development work was performed using CaF_2(Eu) scintillators in the ELEGANT VI system [78].

In the developmental experiments, 25 CaF_2(Eu) crystals with dimensions $4.5 \times 4.5 \times 4.5\,cm^3$ and total mass of 7.2 kg were placed at the centre of the ELEGANT VI array. They were surrounded by CsI (Tl) scintillators and CaF_2 (pure) light pipes to reduce background. The first results from this effort had 9.6×10^{22} ^{48}Ca nuclei and placed a bound of $T^{0\nu}_{1/2} > 1.4 \times 10^{22}$ years (90% CL). This corresponds to an upper bound on the effective Majorana mass of the electron neutrino $\langle m_\nu \rangle$ between 7.2 and 44.7 eV, depending on the nuclear model used. This is far from competitive with the bound from Ge experiments [2, 4, 20]; however, one must keep in mind that the Ca used has a natural abundance of ^{48}Ca of 0.187%.

The half-life sensitivity would have been more than 250 times greater with an isotopic abundance of 50%. To explore the interesting range of neutrino mass implied by the atmospheric neutrino oscillations, the experiment would need $\sim 10^{26}$ ^{48}Ca nuclei. This will require several tons of calcium because of the low natural isotopic abundance of ^{48}Ca.

The new detector system CANDLES employs several tons of calcium in the form of $10 \times 10 \times 10\,cm^3$ CaF_2 (pure) scintillation crystals. The scintillation light from CaF_2, with no Eu doping, is in the ultraviolet (UV) region of the spectrum. It has a rise time of $\sim 1\,\mu s$. They are immersed in a liquid scintillator whose light curve rise-time is a few tens of nanoseconds. The liquid scintillator will act as a background veto, and will contain a wavelength shifting (WLS) component to convert the UV light to the sensitivity of the photomultipliers. It was shown by computational simulation that the energy resolution of such a system could be $\sim 4\%$ at 4.3 MeV.

A complete study of PSD between α-particle and electron scintillation has been done [78]. Based on this, and the other studies, the expected performance parameters are given in table 6 below.

^{238}U contamination of the scintillator is less than $(2\text{–}5) \times 10^{-16}$ g g^{-1}. The inner vessel is made of transparent nylon film, 500 μm thick, which allows one to collect scintillation light with the help of 100 phototubes (8″ Thorn EMI 9351) fixed to a 7 m diameter support structure inside the water tank. The photomultiplier tubes are fitted with light concentrators 57 cm long and 50 cm diameter aperture. It gives a 20% optical coverage.

Table 6. The predicted performance of three future versions of the CANDLES project.

	CANDLES III	CANDLES IV	CANDLES final version
CaF_2 volume	191 kg	~3.2 ton	32 ton or 3.2 ton (2% enriched ^{48}Ca)
Energy resolution	4%	4%	4%
Measurement time	3 years	5 years	5 years
Target Purity (^{214}Bi)	30 μBq kg^{-1}	3 μBq kg^{-1}	<1 μBq kg^{-1}
(^{212}Bi)	30 μBq kg^{-1}	3 μBq kg^{-1}	<1 μBq kg^{-1}
Background rate	0.3 year	0.9 year	
Sensitivity for $\langle m_\nu \rangle$	0.5 eV	0.1 eV	0.03 eV

The values of $\langle m_\nu \rangle$ appearing in the table were computed with the matrix element published by Pantis *et al* [70].

At this point it is interesting to compute the figure-of-merit for such an experiment using the parameters of CANDLES IV. In this case: $\overline{\eta} = 0.54$, $a = 1.87 \times 10^{-3}$, $\epsilon \simeq 0.95$, $W = 78.07$, $M = 3200$ kg, $\delta E = 170.88$ keV and $b = 0.9\,\text{year}^{-1}(171\,\text{keV})^{-1}\,3200\,\text{kg}^{-1} = 1.65 \times 10^{-6}\,\text{keV}^{-1}\,\text{kg}^{-1}\,\text{year}^{-1}$. Substituting these numbers into equation (21), one deduces the figure-of-merit of: $f \simeq 0.04$. Isotopically enriching the calcium to 5% in ^{48}Ca would result in: $f \simeq 1.1$, a very respectable value, if the background rate can be controlled to this level.

Even in this case, the energy resolution, 4%, results in a full-width at half-maximum (fwhm) of ~170 keV. This makes a discovery potential very difficult if only tens of counts are spread over an energy range of ~200 keV, even with this incredible low level of background, 0.9 counts per year in the area of the $0\nu\beta\beta$-decay peak with 3200 kg of detector.

This analysis again shows how important isotopic enrichment and energy resolution are for a next generation $0\nu\beta\beta$-decay experiment with discovery potential.

3.4. The COBRA double-beta decay experiment with CdTe detectors

A $0\nu\beta\beta$-decay experiment involving CdTe ionization detectors has been developed by Zuber [85]; following earlier work [61, 79]. The main isotopes of interest in COBRA are ^{130}Te and ^{116}Cd. This approach will also allow sensitive searches for double-electron capture. A preliminary set up was constructed in the Laboratori Nazionale del Gran Sasso (LNGS) [48].

The CdTe detectors were housed in an active plastic scintillator shield, surrounding a passive lead shield, with a copper shield inside. The copper shield is a $50 \times 50 \times 50$ cm^3 casing of copper inside and lead outside. The passive shield is placed in an airtight $60 \times 60 \times 60$ cm^3 aluminium box flushed with dry nitrogen to minimize the content of ^{222}Rn. The CdTe detectors are inside a special copper brick.

The passive shield is surrounded by 19 plastic scintillators $130 \times 20 \times 0.5$ cm^3 outside the aluminium box. The detection efficiency for cosmic ray muons is 95%.

The energy resolution was measured with various radioactive sources and resulted in the following equations for the named ER and CPG detectors:

$$\triangle E_{ER} = \sqrt{E/\text{keV}} \times 1.68\,\text{keV} + 3.66\,\text{keV}, \tag{25}$$

$$\triangle E_{CPG} = \sqrt{E/\text{keV}} \times 1.03\,\text{keV} - 0.72\,\text{keV}. \tag{26}$$

This implies that the energy resolution at the 2615 keV γ-ray in the decay of ^{208}Tl is ~90 keV for the ER detector and ~52 keV for the CPG detector.

The background in the region 2.7–3.4 MeV was 3.3×10^{-4} keV^{-1} kg^{-1} day^{-1}, which is ~120 keV^{-1} kg^{-1} day^{-1}, ~600 times higher than the background in the ^{76}Ge experiments.

While this technique promises the first measurement of double-electron capture, the energy resolution, and background levels published in [48] will have to be improved significantly for COBRA to be competitive in the search for $0\nu\beta\beta$-decay with $\langle m_\nu \rangle \simeq 40$ meV. Research and development to achieve this improvement continues.

3.5. The drift chamber beta-ray analyser (DCBA)

The DCBA experiment is the only current proposal and active research and development project that plans the use of ^{150}Nd as the parent isotope for a search for $0\nu\beta\beta$-decay. There are several papers that describe the project in significant detail [43, 44, 47].

The instrument is designed to measure the momentum of each beta-ray from the double beta-decay events, and the position of the vertex of the decay. This will allow a three-dimensional reconstruction of the tracks in the uniform magnetic field.

The detector concept is a drift chamber with dimensions $46.4 \times 52.4 \times 68.0$ cm^3 inside of a solenoidal coil with a 72 cm diameter bore and 110 cm in length. The detector will be surrounded by cosmic-ray veto counters.

The energy resolution for a single electron is predicted to be 140 keV for a typical energy of one electron from $0\nu\beta\beta$-decay. The spatial resolution of the vertex of the decay is less than 3 mm. This will greatly assist in the discrimination against background.

There are several phases of the DCBA program: DCBA-T is the construction of a test module for the technical development of the apparatus. The second phase DCBA-I is the construction of a chamber four times the size of DCBA-T, and its operation with a natural isotopic abundance source (5.6% ^{150}Nd). The third phase DCBA-II, will be a chamber 100 times the dimensions of DCBA-II, which they call their standard model (SM). It will operate with natural Nd, ~7.7 moles of ^{150}Nd. The fourth and final phase will be the same chamber operating with Nd isotopically enriched in ^{150}Nd containing 124 moles of ^{150}Nd, or $\sim 7.5 \times 10^{25}$ atoms of ^{150}Nd.

There is only one known practical way to isotopically enrich Nd in kg quantities, that is the AVLIS Process. The only tested facility known to the authors is at the Lawrence Livermore National Laboratory in Livermore, CA. At the time of writing, there is no program there to commercially separate large quantities of isotopes. Neodymium is however a good candidate for this process. It has a favourable atomic energy structure and is refined to be a 'first harmonic' atom for laser ionization.

There are two further concerns. One is the large uncertainly in the nuclear $0\nu\beta\beta$-decay matrix element of ^{150}Nd. This nucleus has a very large static nuclear quadrupole moment. This makes QRPA type calculations very difficult. The other is the 140 keV, single-electron energy resolution. This corresponds to ~200 keV resolution for the $0\nu\beta\beta$-decay events. This makes a discovery experiment extremely difficult, even if an extremely low background is achieved.

In the future, it will be seen if the energy resolution, efficiency and background parameters can be reached that would result in a figure-of-merit of approximately unity.

4. Other proposals involving ^{76}Ge

There are several proposals other than Majorana involving the search for $0\nu\beta\beta$-decay of ^{76}Ge. The Majorana proposal was the only one that is reported completely in this paper because a complete white paper exists and a proposal has been prepared in detail and will be submitted in the near future. The GEM and GENIUS proposals involve operating naked Ge crystals in purified liquid nitrogen [57, 81]. While a very detailed theoretical study has been made of the GENIUS concept and a detailed article written about GEM, no formal proposals for funding have been submitted, nor are expected in the near future. The leader of the GENIUS project has claimed discovery of $0\nu\beta\beta$-decay with a confidence level of 4.1 σ, with a half-life of $\sim 1.2 \times 10^{25}$ years [57]. If this is correct, a full blown GEM or GENIUS project will not be necessary. Nevertheless, these will be discussed later in this section.

There is new proposal, headed by the Max Planck Institute in Heidelberg and Munich, called GERDA. This, as well as the claim of discovery will also be discussed below [64].

4.1. The GEM experiment

The GEM project proposes to construct an array of naked Ge detectors with a mass of $\sim$ 1 ton, emersed in highly purified liquid nitrogen. The first phase, GEM-I proposes to use detectors made with natural abundance germanium, to be followed by GEM-II with 1 ton of Ge detectors made from germanium isotopically enriched to 86% in ^{76}Ge. Detailed Monte Carlo simulations of the backgrounds, and their effect on the experimental sensitivity have been performed. The results imply that with GEM-I, $T^{0\nu}_{1/2} \sim 10^{27}$ years, and $\langle m_\nu \rangle \sim 0.05$ eV, while with GEM-II a half-life of $\sim 10^{28}$ years can be reached with the corresponding sensitivity, $\langle m_\nu \rangle \sim 0.015$. The GEM apparatus could also be used to sensitively search for Cosmic Cold Dark Matter.

A sketch of the general configuration of the GEM apparatus is shown in [81]. The outer dimensions of the water shield are diameter 10 m and height 10 m. The 1 ton of Ge detectors are immersed in a double-wall copper sphere containing 40 tons of liquid nitrogen surrounded by a vacuum jacket.

The radiopurity of the liquid nitrogen is assumed to be the same as that achieved for the liquid scintillator of the BOREXINO experiment: $\sim 10^{-15}$ g g^{-1} of ^{40}K and ^{238}U, and 5×10^{-15} g g^{-1} for ^{232}Th. It has been recently demonstrated by the BOREXINO Collaboration that the liquid scintillator can be purified to $< 5 \times 10^{-16}$ g g^{-1} of ^{232}Th and ^{238}U.

All details of the simulations from which the sensitivity levels were derived for both double beta-decay and Cold Dark Matter are given in [82]. It should be pointed out that the cost of 500 HPGe detectors of about 2 kg, made from p-type, natural abundance germanium would cost roughly one third of the cost of an equal number of enriched detectors. Such an array would be more than adequate to confirm or refute the claim of [52] if the sensitivity calculations are correct.

In any case, this type of study is very useful in helping to formulate a final solution to the problem of observing or putting tight enough bounds on $\langle m_\nu \rangle$ to eliminate the inverted hierarchy or quasi-degenerate neutrino mass eigenstate spectrum.

4.2. The GENIUS project

The GENIUS concept was introduced by Klapdor-Kleingrothaus in the late 1990s and supported by a great deal of computations and experimental research [42], [55]–[57]. A very long and detailed white paper, as well as other articles on the subject, can be found in [57].

The GENIUS project preceded the GEM project, but the two share a number of similar features. The first version would involve 1 ton of HPGe detectors, made from germanium isotopically enriched to 86% in ^{76}Ge, and emersed directly in liquid nitrogen. This proposal was the original naked Ge crystal in liquid nitrogen idea, and proposes a giant tank of LN_2 as the cooling medium and shield. The computations to justify the sensitivity were based on the installation being located in the LNGS (3600 mwe), and used the environmental data on neutron and gamma-ray fluxes measured there.

The optimum size of the LN_2 tank was determined to be a cylinder 12 m in diameter and 12 m high. The naked Ge detectors would be suspended in the centre. These tank dimensions were found to be optimum for shielding the detectors sufficiently from external gamma-ray sources. The neutron flux would first be reduced by 92% by a layer of polyethylene foam outside as a thermal shield and neutron absorber. The remainder would be thermalized in the first 100 cm and captured in the reactions ^{14}N (np)^{14} C* and ^{14}N (nγ)^{15} N*. The γ-ray emissions would still have more than 4 m between the de-exicitation of the carbon and nitrogen nuclei and the germanium detectors.

The muon flux in the LNGS has been measured as $1.1\,\mathrm{m}^{-2}\,\mathrm{h}^{-1}$. The muon flux impact on the background was simulated by placing active veto above the tank with a 96% reduction factor. The total number of neutrons generated by cosmic rays which enter the tank was determined to be $\sim 2.5 \times 10^5\,\mathrm{year}^{-1}$. The two major cosmogenic isotopes produced in the tank would be ^{14}C (5.73×10^3 years) and ^{13}N (9.96 min). These were found to be insignificant contributions to the total background. The construction steel was assumed to be the same as that of the BOREXINO Collaboration which has a level of radiopurity of $5 \times 10^{-9}\,\mathrm{g\,g}^{-1}$ of ^{238}U and ^{232}Th. It was determined that the background from the vessel to the rate in the energy region of $0\nu\beta\beta$-decay (2000–2100 keV) would be $\sim 10^{-4}\,\mathrm{keV}^{-1}\,\mathrm{kg}^{-1}\,\mathrm{year}^{-1}$, where the mass is that of the detector array. The background contributions from the ^{238}U, ^{232}Th, ^{40}K and ^{222}Rd in the LN_2 were evaluated with ^{40}K contributing $\sim 4 \times 10^{-3}\,\mathrm{keV}^{-1}\,\mathrm{kg}^{-1}\,\mathrm{year}^{-1}$, in the region 0–100 keV, with ^{222}Rn contributing $5 \times 10^{-3}\,\mathrm{keV}^{-1}\,\mathrm{kg}^{-1}\,\mathrm{year}^{-1}$ with the other materials contributing enough to have a total of $\sim 10^{-2}\,\mathrm{keV}^{-1}\,\mathrm{kg}^{-1}\,\mathrm{year}^{-1}$ between 10 and 100 keV which is the important energy range for Cold Dark Matter searches.

The simulations imply an expected background in the energy region of $0\nu\beta\beta$-decay of ^{76}Ge ($\sim$2039 keV) to be $5 \times 10^{-5}\,\mathrm{keV}^{-1}\,\mathrm{kg}^{-1}\,\mathrm{year}^{-1}$. The conclusion of Klapdor-Kleingrothaus and co-workers is that a one ton version of GENIUS could reach a sensitivity of $\langle m_\nu \rangle \sim 0.01$ eV in 1 year.

The reader should be careful in accepting the background projections of any of these experiments. They are just that, projections. The projections made for GENIUS, $5 \times 10^{-5}\,\mathrm{keV}^{-1}\,\mathrm{kg}^{-1}\,\mathrm{year}^{-1}$, result in an expectation of:

$$(10^3\,\mathrm{kg})(1\,\mathrm{year})(3.5\,\mathrm{keV})(5 \times 10^{-5}\,\mathrm{keV}^{-1}\,\mathrm{kg}^{-1}\,\mathrm{year}^{-1}) \simeq 0.18\,\mathrm{counts}. \qquad (27)$$

For a null experiment, the statistical laws say there could be 2.3 counts at (90% CL). This would result in a rate of $\sim 6.4 \times 10^{-4}\,\mathrm{keV}^{-1}\,\mathrm{kg}^{-1}\,\mathrm{year}^{-1}$. To a 3σ CL this is more than $10^{-3}\,\mathrm{keV}^{-1}\,\mathrm{kg}^{-1}\,\mathrm{year}^{-1}$. In this case, the maximum half-life sensitivity would be 20 times longer and the sensitivity on $\langle m_\nu \rangle$ would be reduced to 0.04 eV. On the other side of the coin, in the case of an observation, a $0\nu\beta\beta$-decay peak on a zero background does not suffer this statistical disaster.

In conclusion, while the predictions made for sensitivity of the GENIUS experiment are only predictions, and while they appear to be extremely optimistic, the concept is interesting and

merits serious consideration as a good candidate for a next generation $0\nu\beta\beta$-decay technique, also with excellent promise for Cold Dark Matter searches.

4.3. The GENIUS test facility (GENIUS—TF)

The spokesman of the GENIUS project instituted a smaller test project called GENIUS—TF [51]. It involves the immersion and operation of naked Ge detectors in liquid nitrogen. The design plan is to have 14 detectors of approximately 3 kg each in an array of about 40 kg. Thus far, four crystals are operating in the LNGS under these conditions.

They are housed in a steel vessel ∼0.5 mmthick inside of a $0.9 \times 0.9 \times 0.9\,\mathrm{m}^3$ box of high purity Ge bricks. Outside the foam box there will be 10 cm of low-level copper, 30 cm of lead and 15 cm of borated polyethylene.

In the presently operating version, four naked crystals are mounted on a plate made of special Teflon, inside of a thin copper box filled with 70 litres of highly purified liquid nitrogen. The copper is thermally isolated by 20 cm of special low radioactivity styropor, enclosed in a box of 15 tons of electrolytic copper, 10 cm thick and 35 tons of lead 20 cm thick. Outside this high density shield is 10 cm of boron-loaded polyethylene to shield from neutrons. On 5th May 2003, the four crystals began operating, and all reports are that they have been operating without failure to the time of this writing (August/September 2004).

Spectra taken with calibration sources of ^{60}Co and ^{133}Ba are very normal. This technical breakthrough could very well signal a very promising cooling and shielding technique for future ^{76}Ge $0\nu\beta\beta$-decay experiments.

One of the results of interest is that the microphonics from the bubbling of the liquid nitrogen appears to be negligible in the energy region for $0\nu\beta\beta$-decay (2039 keV), however, must be eliminated at low energies of interest in Cold Dark Matter searches, by PSD.

The BOREXINO liquid nitrogen purification system was used in the tests of the facility. GENIUS TF is intended to search for the annual modulation of Cold Dark Matter claimed to have been observed by the DAMA collaboration [23]. While the background in the present set-up is still higher than anticipated, the successful demonstration that p-type naked germanium detectors can be operated for long periods of time directly immersed in liquid nitrogen is a very important technical achievement. The reduction of background and the solution of the problem of operating the field-effect transistors in close proximity to the crystals are technical problems. In principle, Ge detectors can be operated in this manner.

4.4. The new ^{76}Ge experiment at Gran Sasso (GERDA)

Recently, the MPI Heidelberg and MPI Munich-led collaboration introduced a proposal similar to a smaller GENIUS proposal. It involves the direct immersion of Ge detectors, isotopically enriched in ^{76}Ge, directly in either liquid nitrogen or liquid argon. A research pilot program is underway in the MPI laboratories, and engineering has begun on the facility which is planned for the LNGS.

The proposal involves two phases. In the first phase, the 11 kg of detectors from the Heidelberg–Moscow experiment [20, 52] and the 6 kg of detectors from the IGEX experiment [2, 5], are immersed in the well-shielded cryogenic liquid. The plan is to obtain the sensitivity to either refute the recent discovery claim of Klapdor-Kleingrothaus *et al* [52], at a 99.6% CL, or confirm it at the level of 5σ.

In the second phase, the proposal is to measure the half-life to an accuracy of 10% if the claim is correct, or to extend the lower limit on the half-life to 2×10^{26} years if it is not. In this phase, 30 kg of isotopically enriched germanium would be acquired and converted into the maximum mass of detectors.

The first phase of the project has been approved and funded. Construction will begin in early 2005 and data acquisition is scheduled to begin in 2006.

There are negotiations underway between the leadership of the Majorana collaboration and the MPI group that has already led to an agreement to cooperate on various aspects of research and development. Future negotiation will determine if both collaborations will merge to form one large international collaboration for a giant effort in the search for $0\nu\beta\beta$-decay of ^{76}Ge.

4.5. The GSO proposal

This proposal rests on an experimental investigation of $0\nu\beta\beta$-decay of ^{160}Gd with a crystal scintillator of Gd_2SiO_5(Ce), with a volume of 95 cm^3. The experiments were performed in the Solotvina Underground Laboratory (SUL) [31]. In these test experiments, the background was rather high, $\sim$1.0 $keV^{-1}\,kg^{-1}\,day^{-1}$ in the region of the $0\nu\beta\beta$-decay energy, 1730 keV. Most of the background was attributed to ^{208}Tl, ^{212}Bi and ^{212}Po, which presumably could be vastly reduced by purification of the input materials.

The cerium-doped gadolinium silicate crystal, 4.7 cm in diameter by 5.4 cm long, was grown by the Czochralski method; it had a mass of 635 g with 3.95×10^{23} atoms of ^{160}Gd. The SUL has an overburden of $\simeq$1000 mwe. The energy resolution, measured by radioactive calibration sources was 11.2% at 1770 keV, or $\sim$198 keV. The counting efficiency $\epsilon \simeq 0.95$, while the natural abundance of ^{160}Gd is 21.86%. With two small crystals, a lower bound on the half-life is $T^{0\nu}_{1/2} > 1.3 \times 10^{21}$ years (90% CL). This effort is the first step in the development of this technique to investigate the $0\nu\beta\beta$-decay of ^{160}Gd. The isotopic abundance of ^{160}Cd is rather high, 21.86%, therefore a sensitive detector of natural abundance Gd_2SiO_5:Ce scintillators could be constructed. A 2 ton GSO multi- crystal array ($\sim$400 kg of ^{160}Gd) has been predicted to reach the sensitivity of $\langle m_\nu \rangle \sim 0.06$ eV [30].

5. Other proposals involving ^{136}Xe

5.1. The ^{136}Xe experiment in BOREXINO and the BOREXINO test facility

This proposal involves loading the liquid scintillator of the BOREXINO facilities with xenon isotopically enriched in ^{136}Xe [25]. This idea was first developed in an article by R S Raghavan [73]. The BOREXINO experimental facilities are located in Hall C of the LNGS. The BOREXINO main detector has 300 tons of ultrapure liquid scintillator viewed by 2200 photomultipliers and shielded by 3300 tons of radiopure liquids [9]. The scintillator is constantly purified and is maintained at a level of about 10^{-16} g g^{-1} of ^{238}U. It is enclosed in a transparent nylon sphere to separate the scintillator from the shielding liquid.

The BOREXINO experiment is designed to detect the low energy ^{7}Be solar neutrinos and is presently under construction after a long shut down of all activities due to a minor spill of scintillator in 2002 that contaminated water outside of the Gran Sasso Laboratory. Accordingly, if the ^{136}Xe $0\nu\beta\beta$-decay experiment is actually ever done with the BOREXINO detector it will be sometime in the distant future. The original idea of Raghavan was to do this experiment

in the Kamiokande detector, which was subsequently used for the KAMLAND experiment which has for the first time observed oscillations of reactor anti-neutrinos, and confirmed the large mixing angle solution of the solar neutrino problem. This experiment will probably run in its present configuration for some time and would not be available for a ^{136}Xe $0\nu\beta\beta$-decay experiment.

The Sudbury Neutrino Observatory (SNO) will return the deuterated water to the owning Canadian agency in the not very distant future. When that happens, a ^{136}Xe $0\nu\beta\beta$-decay experiment will be considered, along with other scientific uses of the SNO laboratory facilities. Such a possibility has been considered [59].

There is also the possibility of performing this experiment in one of the two BOREXINO test facilities with central chambers of radii 0.5 m (CTF 05) and 1 m (CTF 2). These are also in the Gran Sasso Laboratory.

Two very important parameters are energy resolution and background. A Monte Carlo computation predicts an energy resolution at $Q_{\beta\beta} = 2479\,\mathrm{keV}$ of $\sigma = 79\,\mathrm{keV}$ or fwhm $=$ 186 keV for the full BOREXINO facility and 209 keV for the smaller test facilities.

The final prediction of [25] is that with 80% enriched ^{136}Xe, BOREXINO can achieve a half-life sensitivity of 1.14×10^{27} years. It is straightforward to show that using table 4, one can conclude that to reach a sensitivity of $\langle m_\nu \rangle \sim 40\,\mathrm{meV}$, this experiment needs to reach $\sim 5.8 \times 10^{27}$ years, with the full 1565 kg of Xe dissolved in the scintillator, and with no background.

From table 2 of [25] there are 81 background counts predicted for 1 year of running of the full BOREXINO experiment. This is equivalent to $b \simeq 0.0003\,\mathrm{keV}^{-1}\,\mathrm{kg}^{-1}\,\mathrm{year}^{-1}$. They quote an efficiency of 68%, hence this experiment has the predicted parameters: $a = 0.80$, $\overline{\eta} = 0.28$, $\epsilon = 0.68$, $W = 136$, $M = 1565\,\mathrm{kg}$, $\delta E = 186\,\mathrm{keV}$ and $b = 0.0003\,\mathrm{keV}^{-1}\,\mathrm{kg}^{-1}\,\mathrm{year}^{-1}$. The figure-of-merit is $f = 0.19$. The second figure-of-merit f_d reflecting the signal-to-noise ratio is $f_d = 0.02$. For comparison we quote f_d for a ^{76}Ge experiment with 500 kg, and with a background reduction of only a factor of 10 below the Heidelberg–Moscow or IGEX experiments, i.e., $b = 0.01$. In this case, $f = 0.73$ and $f_d \simeq 0.18$. These parameters speak for themselves. Excellent energy resolution must be complimented by very low background, even in the case of a large mass experiment with high isotopic enrichment and good counting efficiency. The main weakness of this idea is the small mass and poor energy resolution. At the time of its conception (1994), it made sense was a clever innovation. However, at this point, much more sensitivity is required.

5.2. The XMASS experiment

The XMASS project is in the research and development phase. It is a liquid Xe experiment with the goal of observing ^{7}Be solar neutrinos from the pp-chain in real time, direct-observation of Cold Dark Matter (CDM) and the observation and measurement of the $0\nu\beta\beta$-decay of ^{136}Xe [80].

A test cryostat has been built and tested. It has 30 $\mathcal{L}$ of liquid Xe in a 30 cm cubic chamber surrounded by photomultiplier tubes which give a photocathode surface coverage of 16%. The scintillation light output of liquid Xe is $\sim 4.2 \times 10^4$ photons MeV^{-1}, approximately the same as NaI(Tl). The background in this test detector is $\sim 3 \times 10^{-2}\,\mathrm{keV}^{-1}\,\mathrm{kg}^{-1}\,\mathrm{day}^{-1}$ at 2479 keV $\simeq Q_{\beta\beta}$, or $\sim 11\,\mathrm{keV}^{-1}\,\mathrm{kg}^{-1}\,\mathrm{year}^{-1}$. This is rather high; however, it will certainly be reduced in the 800 kg full version of XMASS, because the fiducial volume mass of 100.5 kg will be well shielded by $\sim$700 kg of Xe.

Let us assume that the isotopic abundance is the canonical 80% and the efficiency is the photocathode coverage ∼70%. We can estimate an improvement in the energy resolution measured in the 100 kg version (580 keV) by the ratio of the photocathode coverage of the two configurations, i.e. $0.16/0.70 = 0.229$. This yields $\delta E \sim 133$ keV. Let us assume that the background in the 100 kg test cryostat, 11 keV^{-1} kg^{-1} year^{-1} can be reduced by a factor of 1000 in the fiducial volume of the 800 kg detector. Then the estimated parameters for this configuration are: $\overline{\eta} = 0.28$, $a = 0.80$, $\epsilon = 0.70$, $W = 136$, $M = 800$ kg, $\delta E = 133$ keV and $b \simeq 0.011$. The resulting figure-of-merit, $f = 0.04$.

If on the other hand, the background is reduced by a factor of 10^{-4}, then $f = 0.09$. To achieve a figure-of-merit of unity, the background must be reduced to the very challenging level of $\sim 10^{-5}$ keV^{-1} kg^{-1} year^{-1}.

Certainly a 10 ton version will have a much better figure-of-merit since the fiducial volume will be far better shielded and M will be 12.5 times larger. For $0\nu\beta\beta$-decay, this is a very challenging experiment. Nevertheless, XMASS will have to experience great improvements to be competitive with those proposals with $f \simeq 1$. As for its other applications it might well be a very effective and competitive experiment. The figure-of-merit applied above only applies to $0\nu\beta\beta$-decay.

6. The figure-of-merit revisited

The computation of the figure-of-merit proposed in equation (21) has one parameter that is difficult to justify in many cases; that is the background rate b in keV^{-1} kg^{-1} year^{-1}. The rest of the parameters are usually fairly well established. Another use of this equation is to make a conserverative assumption about any experiment with respect to its probable background reduction. For this we choose the Majorana experiment and choose the parameters given in tables 2–4 of the Majorana White Paper [60]. Much of the data is dependent on more than 20 years of development of the PNNL/Carolina and IGEX experiments. The results are similar for the Heidelberg–Moscow Experiment [20]. We take the projected total background rate and multiply it by a factor of 2 to make it more conservative. Direct substitution into equation (19) results in f (Majorana) $= 1$. If instead we say that the Majorana array will conservatively have only 10 times lower background than IGEX with PSD, 0.11, then $b \simeq 0.01$. In this case $f = 0.79$. So we use the similar $f = 1$ value and compare experiments to this canonical value of unity. We can then use equation (28) to determine the background level that must be achieved for an experiment to have $f \simeq 1$. In this case,

$$b = \frac{M}{\delta E}\left(\frac{\overline{\eta} a \epsilon}{W}\right). \tag{28}$$

Let us apply this to CUORE operating with 760 kg of TeO_2 bolometers with natural abundance Te (33.8% ^{130}Te). In this case $b \leqslant 0.0058$ keV^{-1} kg^{-1} year^{-1}. For a completely isotopically enriched CUORE (∼85% ^{130}Te), this becomes $b \leqslant 0.009$, which is a factor of 22 below that already reached by CUORICINO. Research and development is underway to reduce the background which is now understood from the CUORICINO results.

This is a more realistic way to compare the competitiveness of a given proposal, rather than to accept backgrounds predicted by Monte Carlo calculations and models that are different for every proposal, and in some cases not supported by sufficient experimental data.

Finally, while equation (21) is very useful for gaining a general idea of the merits of any given proposed experiment, it has somewhat of a shortcoming in evaluating its discovery potential. For this purpose we consider a rather unconventional parameter in this application, f_d, which is directly proportional to the signal-to-background ratio. This is simply derived as follows:

$$f_d \equiv \frac{\lambda N t \epsilon}{bM\delta Et} \propto \frac{\overline{\eta}(A_0 \times 10^3) Ma\epsilon t}{WbM\delta Et} \propto \frac{\overline{\eta} a \epsilon}{Wb\delta E}. \tag{29}$$

This parameter emphasizes the importance in the background as well as the energy resolution in being able to make a positive statement of discovery. Equations (21) and (28) emphasize different merits of an experiment. Equation (21) emphasizes how high the counting efficiency is, and how many atoms of the parent there are, whereas equation (29) gives some indication of how easy/difficult it will be to pick the needle of discovery from the haystack of background. It is clear that f_d makes no sense when $b \to 0$, but that is a case in which no such approach is necessary. In addition, the cancellation of the source mass in equation (29) clearly implies that two experiments with vastly different masses can not be compared this way.

6.1. The claim of discovery of $0\nu\beta\beta$-decay of ^{76}Ge

In 2001, a report of evidence of the direct observation of the $0\nu\beta\beta$-decay of ^{76}Ge was published by Klapdor-Kleingrothaus *et al* [50]. Several critical papers followed pointing out 'soft spots' in the analysis [2, 38]. Since that time two new papers have been published by Klapdor-Kleingrothaus *et al* which give a new analysis, and many new experimental details as well [52, 53].

In this latest paper, [53], 71.7 kg year of data from the Heidelberg–Moscow experiment was analysed. The background rate was 0.11 $\mathrm{keV}^{-1}\,\mathrm{kg}^{-1}\,\mathrm{year}^{-1}$. The authors of this paper are members of the collaboration and have done extensive analysis and have concluded that the most probable half-life for the $0\nu\beta\beta$-decay of ^{76}Ge is 1.19×10^{25} years, and that the signal corresponds to a positive observation at a level of confidence of 4.2σ. The 3σ range of half-life values is $(0.69\text{–}4.18) \times 10^{25}$ years and it corresponds to the range in effective Majorana mass of the electron neutrino $\langle m_\nu \rangle$ of (0.24–0.58) eV, with the best-fit value $\langle m_\nu \rangle = 0.44$ eV. In this analysis, the nuclear matrix elements of Staudt *et al* were used [75]. Using the mean value from the literature for nuclear structure factor, $F_N = 7.3 \times 10^{-14}\,\mathrm{year}^{-1}$, the parameter $\langle m_\nu \rangle$ has the range 0.29–0.72 eV, with the value corresponding to the best fit half-life of 0.55 eV, not vastly different from the value obtained by the original authors.

One notes that the authors of this paper represent only a small part of the Heidelberg–Moscow Collaboration. In fact, the Russian component of the collaboration presented a conflicting view of the interpretation [22].

Since there appears much literature supporting or refuting this issue, we shall not argue either side. Although the interpretation of the data which leads to the conclusion of a discovery is highly controversial, the high quality of the Heidelberg–Moscow experiment, and its resulting data are not being questioned by anyone. It is our conclusion that the only completely reliable way to settle this issue is to test it experimentally.

There is only one experiment running at this time that would have a sensitivity anywhere near that required to confirm this claim, and that is CUORICINO. Unfortunately, this experiment will have the capability of refuting only part of the claimed range of $\langle m_\nu \rangle$ because of the uncertainty in the nuclear matrix elements. The new planned effort by the Max Planck Institute will test it in the next 4–5 years and so will the CUORE and Majorana experiments discussed earlier.

The IGEX experiment published a lower bound: $T^{0\nu}_{1/2} \geqslant 1.6 \times 10^{25}$ years (90% CL), which corresponds to $\langle m_\nu \rangle \leqslant 0.38$ eV, using the matrix elements of [75]. This experiment can not rule out most of the claimed range of $T^{0\nu}_{1/2}$, but has been attacked by Klapdor-Kleingrothaus *et al* as having serious flaws, mainly an arithmetical error that leads to a bound on the half-life far below their claim [54]. This has been responded to by the IGEX collaboration [4] completely answering all questions, and in particular, clearly demonstrating that there is no arithmetical error, and will appear alongside [54].

6.2. Figure-of-merit for a sample ^{76}Ge experiment

There are several proposals for ^{76}Ge $0\nu\beta\beta$-decay experiments utilizing Ge detectors isotopically enriched to 86% in ^{76}Ge. We can use the Majorana proposed experimental parameters as an example [60]. The parameters are as follows: $M = 500\,\text{kg}$, $\delta E = 3.5\,\text{keV}$, $\overline{\eta} = 0.73$, $\epsilon = 0.75$ (after pulse-shape analysis and segmentation cuts), $W = 76$, $a = 0.86$ and $b = 0.0028\,\text{keV}^{-1}\,\text{kg}^{-1}\,\text{year}^{-1}$. The background rate was determined from the Majorana White Paper in which it is stated that after 2500 kg year, and after applying pulse-shape discrimination and cuts due to multiple interactions in a segmented detector, there would remain seven background events. Accordingly,

$$f = \frac{(0.73)(0.86)(0.75)}{76}\sqrt{\frac{500}{(0.0028)(3.5)}} = 1.40. \tag{30}$$

This form of figure-of-merit is good guidance for selecting a technique and an isotope; however, it does not give enough weight to the energy resolution in evaluating the discovery potential. It is straight forward to show that the signal-to-noise ratio is proportional to $f_d = \overline{\eta}/b\delta E$, which is the second type of figure-of-merit discussed earlier. In detection techniques with 10s or 100s of keV energy resolution, the background must be reduced enormously to compensate. Computing f_d in this case, we see $f_d \simeq 0.63$ which is very superior to the cases discussed above. This is an extremely important figure-of-merit when considering discovery potential.

6.3. The CUORE proposal with natural abundance TeO_2 bolometers

The CUORE proposal involves 1000, 760 g TeO_2 bolometers operated at $\sim$10 mK. A complete description is given by Arnaboldi *et al* [13]. A pilot experiment, CUORICINO, constituting about 1/24 of CUORE has been operated successfully in the Gran Sasso Laboratory [12]. It has the following parameters: $M = 760\,\text{kg}$, $\delta E = 7\,\text{keV}$, $\overline{\eta} = 4.2$, $a = 0.338$, $\epsilon = 0.84$, $W = 163$ and $b = 0.01\,\text{keV}^{-1}\,\text{kg}^{-1}\,\text{year}^{-1}$. This value of b was derived by reducing the background of CUORICINO by a conservative factor of 20, using the computed background cancellation factor employing anti-coincidence cancellation of gamma-ray background events, and the shielding effect of the outter TeO_2 crystals, as well as material quality control.

Substituting these parameters into equation (20) yields $f = 0.76$. If CUORE were to be constructed of bolometers of TeO_2 isotopically enriched to 85% in ^{130}Te, the figure-of-merit would be $f = 1.9$.

One should be cautious in evaluating these competing experimental approaches because they are very sensitive to background rates, and those used above have been calculated by the proponents of the various proposals or estimated by these authors, based on target values in the

various proposals. They may or may not ever be achieved. Nevertheless, we can clearly see that experiments involving ^{76}Ge and bolometer-type experiments yield very superior figures of merit and discovery potential. This fact is mainly due to superior energy resolutions.

6.4. Figure-of-merit for a 10 ton ^{136}Xe TPC

Let us estimate the figure-of-merit for a 10 ton TPC with some of the parameters of the EXO experiment, and some estimated from assumed improvements one might make in those from the Gotthard Tunnel experiment [58]. From that paper we estimate that in 1.465 years of operation, with 24.2 moles of ^{136}Xe, they had ∼7 background counts in the 163 keV energy interval of interest. Let us further assume that the background $b = 0.043$ can be improved by a factor of 100, such that $b = 0.00043\,\mathrm{keV}^{-1}\,\mathrm{kg}^{-1}\,\mathrm{year}^{-1}$. The energy resolution in tests of EXO yield 2% at the $0\nu\beta\beta$-decay energy of 2479 keV. Let us also use the isotopic enrichment planned for EXO of 80%. We will also use the efficiency of the Gotthard experiment, 30%. The figure-of-merit is then estimated as follows:

$$f = \frac{(0.28)(0.80)(0.30)}{136}\sqrt{\frac{10000\,\mathrm{kg}}{(0.00043\,\mathrm{keV}^{-1}\,\mathrm{kg}^{-1}\,\mathrm{year}^{-1})(50\,\mathrm{keV})}} \simeq 0.34. \quad (31)$$

In order to make this figure-of-merit greater than unity, the background would have to be reduced by a factor of 1000 below that of the Gotthard experiment, or $4.3 \times 10^{-5}\,\mathrm{keV}^{-1}\,\mathrm{kg}^{-1}\,\mathrm{year}^{-1}$. This is a factor of 70 better than that projected for the Majorana ^{76}Ge experiment, $(0.003\,\mathrm{keV}^{-1}\,\mathrm{kg}^{-1}\,\mathrm{year}^{-1})$ and a factor of ∼2560 lower than the lowest ever achieved with Ge detectors with pule-shape discrimination [1, 39, 53, 60]. While conceivable if the positive identification of the daughter ^{136}Ba^{+} is successful, it will require this drastic improvement to be competitive. The background will have to be reduced to $b = 7.5 \times 10^{-5}\,\mathrm{keV}^{-1}\,\mathrm{kg}^{-1}\,\mathrm{year}^{-1}$ to match the discovery potential figure-of-merit f_d of a ^{76}Ge experiment with the parameters of Majorana.

In this section, we have tried to be as objective as possible; however, it is possible that our prejudice in favour of experimental approaches that feature excellent energy resolution has shown through. As stated in the beginning, no experimental proposal has all of the features that make an ideal neutrinoless double-beta decay experiment. All of the various proposals are clever but some have features that would only have made sense a few years ago. Recently, however, neutrino oscillation experiments give a clear indication of the required sensitivity of an experiment with discovery potential.

7. Conclusion

In this paper, we have recommended and applied two somewhat novel figure-of-merit formulae for use in comparing the relative merits of different $0\nu\beta\beta$-decay proposals. The first is similar to others used for many years but different in one important aspect. It is proportional to the ratio of the predicted experimental sensitivity to the average theoretically calculated half-life for some arbitrary value of the Majorana mass of the electron neutrino. This is achieved by multiplying the usual expression for the figure-of-merit by $\overline{\eta}$, the average of the theoretical values of $G^{0\nu}|M^{0\nu}|^2 \times 10^{13}\,\mathrm{year}^{-1}$. Multiplying by the arbitrary factor 10^{13} simply yields values of order unity for convenience.

The second figure-of-merit, although unconventional, is a better measure of the experiment's ability to produce data that would lend itself to an analysis to identify a positive peak signalling the identification of $0\nu\beta\beta$-decay. This quantity is proportional to the ratio of the theoretically predicted signal, which is proportional to $\overline{\eta}$, and the expected background. It places more emphasis on the impact of energy resolution and background. It is obviously invalid for $b = 0$.

Fifteen proposals that are carefully documented in published papers and reports are discussed in some detail. Five proposals: CUORE, EXO, Majorana, MOON and NEMO/Super-NEMO are discussed in more detail because extensive research, development and documentation from previous experiments appear in the literature. Ten other experiments: CARVEL, CANDLES, DCBA, GEM, GENIUS, GENIUS-TF, GERDA, GSO, Xe (in BOREXINO) and XMASS, are discussed in enough detail to allow the reader to attempt to evaluate to some degree the figures of merit discussed in this paper.

We do evaluate a few examples in cases in which enough data are available. We do not present a table comparing the various proposals, because in most cases the background predictions are too poorly documented, and in many cases very uncertain. Tables tend to be quoted with none of the caveats of the accompanying text.

Two experimental techniques with excellent energy resolutions, cryogenic bolometers (CUORE), and Ge ionization detectors (Majorana, GEM, GENIUS and GERDA) will all have significant discovery potential if they achieve their target background levels. These experiments all have earlier versions that give some level of confidence that the steps necessary to reach the stated background goals are understood.

The canonical target experimental sensitivity for next generation experiments is chosen as the half-life that corresponds to the effective Majorana mass of the electron neutrino $\langle m_\nu \rangle \sim 0.04$ eV. This is approximately the minimum value implied by the measured atmospheric neutrino oscillation parameters in the case of the inverted neutrino mass eigenstate hierarchy.

The statements made above favouring bolometers and Ge detectors, are not intended to exclude the rest of the proposals. Tracking detectors, for example, could explore $0\nu\beta\beta$-decay of ^{150}Nd, for which at present there is no known ionization detector or bolometer. While tracking detectors do not have good energy resolution, NEMO, for example has shown that backgrounds can be identified and drastically reduced. Tracking detectors can also exploit the large value of $\overline{\eta}$ (^{100}Mo), which is almost seven times larger than that of ^{76}Ge, and slightly larger than that of ^{130}Te. In this regard, it would also be very worthwhile to attempt the development a bolometer containing a significant amount of ^{100}Mo because $|Q_{\beta\beta}| = 3034$ keV, above the natural radioactive γ-ray background. Such a project is underway in the CUORE collaboration.

The measured parameters from neutrino oscillation experiments strongly imply a large discovery area in $\langle m_\nu \rangle$—m_1 parameter space that allows values of $\langle m_\nu \rangle$ from 0.04 eV to the present bounds, and also include the range of the claim of discovery of Klapdor-Kleingrothaus *et al*.

Finally, these are very exciting times for those of us who have been working on double-beta decay for many years. There is the feeling that a confirmed discovery may be just around the corner.

Acknowledgments

The authors are grateful to S Elliott for reviewing the manuscript and for his many helpful comments. They also wish to thank Professors H Ejiri, G Gratta, and S Julian for their help

in preparing the sections and figures for the MOON, EXO and NEMO sections, respectively. Following the last corrections to this text, our colleague and co-author Y G Zdesenko passed away suddenly on 1 September 2004. We dedicate this paper to his memory. All who knew him will miss his intense interest and enthusiasm in the science of our field.

References

[1] Aalseth C E 2000 *PhD Dissertation* University of South Carolina
[2] Aalseth C E *et al* 2002 *Phys. Rev.* D **65** 092007
[3] Aalseth C E *et al* 2002 *Mod. Phys. Lett.* A **17** 1475
[4] Aalseth C E *et al* 2004 *Preprint* nucl-ex/0404036
Aalseth C E *et al* 2004 *Phys. Rev.* D **70** 078302
[5] Aalseth C E *et al* 1999 *Phys. Rev.* C **59** 2108
[6] Ahmad Q R *et al* (The SNO Collaboration) 2001 *Phys. Rev. Lett.* **87** 071301
Ahmad Q R *et al* 2004 *Phys. Rev. Lett.* **92** 181301
[7] Alessandrello A *et al* 1997 *IEEE Trans. Nucl. Sci.* **44** 416
[8] Alessandrello A *et al* 1998 *Nucl. Instrum. Methods* A **142** 454
[9] Alimonti G *et al* 1998 *Nucl. Instrum. Methods* A **406** 411
[10] Apollonio M *et al* (The CHOOZ Collaboration) 1999 *Phys. Lett.* B **466** 415
[11] Arnaboldi C *et al* 2003 *Phys. Lett.* B **557** 167
[12] Arnaboldi C *et al* 2004 *Phys. Lett.* B **584** 260
[13] Arnaboldi C *et al* 2004 *Nucl. Instrum. Methods* A **518** 775
[14] Arnold R *et al* 1996 *Z. Phys.* C **72** 239
[15] Arnold R *et al* 2003 *Nucl. Instrum. Methods* A **503** 649
[16] Avignone F T III and Brodzinski R L 1988 *Prog. Part. Nucl. Phys.* **21** 99
[17] Avignone F T III and King G S III 2003 *Proc. 4th Int. Workshop on Identification of Dark Matter* (York 2002) ed N J Spooner and V Kudryatsev (Singapore: World Scientific), p 553 (and references therein)
[18] Bahcall J N, Gonzales-Garcia M C and Pena-Garay C 2002 *Preprint* hep-ph/0204314 and 0204194
[19] Barger V, Glashow S L, Marfatia D and Whisnant K 2002 *Phys. Lett.* B **532** 15
[20] Baudis L *et al* 1999 *Phys. Rev. Lett.* **83** 41
[21] Bellini G *et al* 2000 *Phys. Lett.* B **493** 216
Bellini G *et al* 2001 *Eur. Phys. J.* C **19** 43
[22] Belyaev S T 2003 *Invited talk at the IV Int. Conf. on Non-Accelerator New Physics (NANP-03; June 23–28, Dubna) Yad. Fiz.* at press
[23] Bernabei R *et al* 2000 *Phys. Lett.* B **480** 23
[24] Boehm F *et al* 2001 *Phys. Rev.* D **64** 112001
[25] Caccianiga B and Giammarchi M G 2000 *Astropart. Phys.* **14** 15
[26] Ling-Lie Chau and Wai-Yee Keung 1984 *Phys. Rev. Lett.* **53** 1802
[27] Civaterese O and Suhonen J 2002 *Preprint* nucl-th/0208005
[28] Danilov M *et al* 2000 *Phys. Lett.* B **480** 12
[29] Danevich F A *et al* 2000 *Phys. Rev.* C **62** 045501
[30] Danevich F A *et al* 2001 *Nucl. Phys.* A **694** 375
[31] Danevich F A *et al* 2003 *Phys. Rev.* C **68** 035501
[32] Ejiri H *et al* 2000 *Phys. Rev.* C **63** 065501
[33] Ejiri H, Engle J and Kudomi N 2001 *Preprint* astro-ph/0112379
[34] Elliott S R and Vogel P 2002 *Annu. Rev. Part. Sci.* **52** 115
[35] Elliott S R and Engel J 2004 *Preprint* hep-ph/0405078
Elliott S R and Engel J 2004 *J. Phys. G: Nucl. Part. Phys.* **30** R 183
[36] Fakuda S *et al* (The SuperKamiokande Collaboration) 2002 *Phys. Lett.* B **539** 179

[37] Fakuda S *et al* (The SuperKamiokande Collaboration) 1998 *Phys. Rev. Lett.* **81** 1562
Fakuda S *et al* (The SuperKamiokande Collaboration) 1999 *Phys. Rev. Lett.* **82** 2644
[38] Feruglio F, Strumia A and Vissani F 2002 *Nucl. Phys.* B **637** 345
[39] Gonzales D *et al* (The IGEX Collaboration) 2003 *Nucl. Instrum. Methods* A **515** 634
[40] Grigoriev G and Karchevsky A 2001 *Proc. 3rd Int. Conf. on Non-Accelerator New Physics (NANP-2001; June 19–23, Dubna)* (http://nanp.dubna.ru)
[41] Haxton W C and Stephenson G J Jr 1984 *Prog. Part. Nucl. Phys.* **12** 409
[42] Hellmig J and Klapdor-Kleingrothaus H V 1997 *Z. Phys.* A **359** 372
[43] Ishihara N *et al* 2001 *Nucl. Instrum. Methods* A **433** 101
[44] Ishihara N *et al* 2002 *Nucl. Phys.* B (Proc. Suppl.) **111** 309
[45] Kajita T (The SuperKamiokande Collaboration) 1999 *Nucl. Phys.* (Proc. Suppl.) **77** 123
[46] Eguchi K *et al* (The KAMLAND Collaboration) 2004 *Phys. Rev. Lett.* **92** 071301 (*Preprint* hep-ex/0406035)
[47] Kato Y *et al* 2003 *Nucl. Instrum. Methods* A **498** 430
[48] Kiel H, Munstermann D and Zuber K 2003 *Nucl. Phys.* A **723** 499
[49] Klapdor-Kleingrothaus H V *et al* 2001 *Eur. Phys. J.* A **12** 147
[50] Klapdor-Kleingrothaus H V, Deitz A, Harney H L and Krivosheina I V 2001 *Mod. Phys. Lett.* **16** 2409
[51] Klapdor-Kleingrothaus H V 2003 Naked crystals go underground *Preprint* hep-ph/0307329
[52] Klapdor-Kleingrothaus H V, Krivosheina I V, Dietz A and Chkvorets O 2004 *Phys. Lett.* B **586** 198
[53] Klapdor-Kleingrothaus H V, Krivosheina I V, Dietz A and Chkvorets O 2004 *Nucl. Instrum. Methods* **522** 367 (see many Klapdor-Kleingrothaus references therein)
[54] Klapdor-Kleingrothaus H V, Dietz A and Krivosheina I V 2004 *Phys. Rev.* D, at press (*Preprint* hep-ph/0403056)
[55] Klapdor-Kleingrothaus H V and Hirsch M 1997 *Z. Phys.* A **359** 361
[56] Klapdor-Kleingrothaus H V 1997 *CERN Courier* (Dec.) 19
[57] Klapdor-Kleingrothaus H V, Hellmig J and Hirsch M 1998 *J. Phys. G: Nucl. Part. Phys.* **24** 483
For a complete white paper see Klapdor-Kleingrothaus H V *et al* 2000 *Preprint* hep-ph/991 0205 V4
[58] Luescher R *et al* 1998 *Phys. Lett.* B **434** 407
[59] McDonald A 2000 private communication
[60] The Majorana White Paper 2003 *Preprint* Nucl.ex//0311013
[61] Mitchel L V and Fisher P H 1988 *Phys. Rev.* C **38** 895
[62] Moe M K 1991 *Phys. Rev.* C **44** R 931
[63] Moe M and Vogel P 1994 *Ann. Rev. Nucl. Part. Sci.* **44** 247
[64] Abt I *et al* 2004 A new ^{76}Ge double-beta decay experiment at LNGS' Max Planck Institute letter of intent *Preprint* hep-ex/040 4039 V1
[65] Neuhauser W *et al* 1978 *Phys. Rev. Lett.* **41** 233
[66] Osipowicz A *et al* 2001 (The KATRIN collaboration) *Preprint* hep-ex/0109033
Drexlin G 2004 Helmholtz-Gemeinschaft (HGF) Pre-Meeting, Forschungszentrum Karlsruhe
[67] Pascoli S and Petcov S T 2002 *Phys. Rev.* D *Preprint* hep-ph/0205022
[68] Pascoli S and Petcov S T 2003 *Preprint* hep-ph/031 0003 Vi
[69] Pessina G 1999 *Rev. Sci. Instrum.* **70** 3473
[70] Pantis G *et al* 1992 *J. Phys. G: Nucl. Part. Phys.* **18** 605
[71] Primakoff H and Rosen S P 1969 *Phys. Rev.* **184** 1925
[72] Primakoff H and Rosen S P 1981 *Ann. Rev. Nucl. Part. Sci.* **31** 145
[73] Raghavan R S 1994 *Phys. Rev. Lett.* **72** 1411
[74] Rodin V A, Faessler A, Simkovic F and Petr Vogel 2003 *Phys. Rev.* C **68** 044302
[75] Staudt A, Muto K and Klapdor-Kleingrothaus H V 1990 *Europhys. Lett.* **13** 31
[76] Tomei C, Dietz A, Krivosheina I and Klapdor-Kleingrothaus H V 2003 *Preprint* hep-ph/0306257
[77] Tretyak V I and Zdesenko Yu G 2002 *At. Data Nucl. Data Tables* **80** 83
[78] Umehara S *et al* 2003 *Proc. 1st Yamada Symp. on Neutrinos and Dark Matter in Nucl. Phys.* (http://ndm03.phys.sci.osaka-u.ac.jp/proc/index.htm) XII-23

[79] Watanabe T *et al* 1990 *Nucl. Instrum Methods* A **436** 155
[80] Moriyama S 2001 (For the XMASS collaboration) *Proc. Int. Workshop on Techniques and Applications of Xenon Detectors (Tokyo, Japan, 3–4 December)* (Singapore: World Scientific) p 123; see also http://www-sk.icrr.u-tokyo.ac.jp/∼minamino/doc/KEKPH_Mar_2004.pdf
[81] Zdesenko Yu G, Ponkratenko O A and Tretyak V I 2001 *J. Phys. G: Nucl. Part. Phys.* **27** 2129
[82] Zdesenko Yu G 2002 *Rev. Mod. Phys.* **74** 663
[83] Zdesenko Yu G *et al* 2004 *Nucl. Instrum. Methods* at press (*INR Kiev Preprint*)
[84] Zdesenko Yu G *et al* 2004 *J. Phys. G: Nucl. Part. Phys.* **30** 971
[85] Zuber K 2001 *Phys. Lett.* B **519** 1